(4)

AFGL-TR-87-0256

Ultrasonic Physical Modeling of Seismic Wave Propagation from Graben-Like Structures

M.S. Vassiliou
M. Abdel-Gawad
B.R. Tittmann

Rockwell International Science Center
1049 Camino Dos Rios
Thousand Oaks, CA 91360

November 1987

Final Report
19 February 1985 - 30 June 1987

APPROVED FOR PUBLIC RELEASE; DISTRIBUTION UNLIMITED

AIR FORCE GEOPHYSICS LABORATORY
AIR FORCE SYSTEMS COMMAND
UNITED STATES AIR FORCE
HANSCOM AIR FORCE BASE, MASSACHUSETTS 01731-5000

Sponsored by:
Defense Advanced Research Projects Agency
Nuclear Monitoring Research Office
DARPA Order No. 5307

Monitored by:
Air Force Geophysics Laboratory
Under Contract No. F19628-85-C-0034

"This technical report has been reviewed and is approved for publication."

JAMES F. LEWKOWICZ
Contract Manager

HENRY A. OSSING
Chief, Solid Earth Geophysics Branch

FOR THE COMMANDER

DONALD H. ECKHARDT
Director
Earth Sciences Division

UNCLASSIFIED

SECURITY CLASSIFICATION OF THIS PAGE

REPORT DOCUMENTATION PAGE

1a. REPORT SECURITY CLASSIFICATION UNCLASSIFIED	1b. RESTRICTIVE MARKINGS
2a. SECURITY CLASSIFICATION AUTHORITY	3. DISTRIBUTION/AVAILABILITY OF REPORT Approved for public release; distribution unlimited
2b. CLASSIFICATION/DOWNGRADING SCHEDULE	
4. PERFORMING ORGANIZATION REPORT NUMBER(S) SC5420.FR	5. MONITORING ORGANIZATION REPORT NUMBER(S) AFGL-TR-87-0256
6a. NAME OF PERFORMING ORGANIZATION ROCKWELL INTERNATIONAL Science Center 6b. OFFICE SYMBOL (If Applicable)	7a. NAME OF MONITORING ORGANIZATION Defense Advanced Research Projects Agency
6c. ADDRESS (City, State, and ZIP Code) 1049 Camino Dos Rios Thousand Oaks, CA 91360	7b. ADDRESS (City, State and ZIP Code) 400 Wilson Blvd. Arlington, VA 22209
8a. NAME OF FUNDING/SPONSORING ORGANIZATION Solid Earth Geophysics Branch Earth Sciences Division 8b. OFFICE SYMBOL (If Applicable)	9. PROCUREMENT INSTRUMENT IDENTIFICATION NUMBER CONTRACT NO. F19628-85-C-0034
8c. ADDRESS (City, State and ZIP Code) Department of the Air Force Air Force Geophysics Laboratory (AFSC) Hanscom AFB, MA 01731	10. SOURCE OF FUNDING NOS.

10. SOURCE OF FUNDING NOS.

PROGRAM ELEMENT NO.	PROJECT NO.	TASK NO.	WORK UNIT NO.
62714E	5A10	DA	AU

11. TITLE (Include Security Classification)
ULTRASONIC PHYSICAL MODELING OF SEISMIC WAVE PROPAGATION FROM GRABEN-LIKE STRUCTURES

12. PERSONAL AUTHOR(S)
Vassiliou, M.S., Abdel-Gawad, M., Tittmann, B.R.

13a. TYPE OF REPORT	13b. TIME COVERED	14. DATE OF REPORT (Yr., Mo., Day)	15. PAGE COUNT
Final Report	FROM 02/19/85 TO 06/30/87	1987, NOVEMBER	50

16. SUPPLEMENTARY NOTATION

17. COSATI CODES			18. SUBJECT TERMS (Continue on reverse if necessary and identify by block number)
FIELD	GROUP	SUB. GR.	Ultrasonic, experiments, point source, transducers, seismic waves, Rayleigh waves, modeling, 3-D models, waveforms, velocity, amplitude, propagation, scattering, frequency spectra, half-space, geologic structure, graben, Yucca Flat, nuclear testing, Nevada Test Site

19. ABSTRACT (Continue on reverse if necessary and identify by block number)

are produced sub P

This report describes ultrasonic experiments intended to help clarify the problem of seismic wave propagation in cases where sources are excited in a graben-like structure with significantly different material properties from those of the surrounding propagation medium. ~~We produced~~ ultrasonic waves using a breaking pencil lead as a source (step unloading of the surface) and a true-displacement conical transducer as a receiver. We have made measurements by exciting the source on the half space (made of fine grained gabbro, with $V_p = 6.2$ km/s) and within two graben-like structures: a cylindrical plug "graben" of 13 mm diameter and 2 mm depth; and a scale model (1 mm = 1 km) of Yucca Flat. The structures were filled with either Crystalbond 504 (Aremco Products, Inc.; $V_p = 2.407$) or HPAL3 (an aluminum-filled resin with $V_p = 3.287$).

In the case of cylindrical graben, the presence of a source region with significantly slower velocities than the surrounding region appears to lead to a more complex signal, with more "ringing" than would be apparent if there were no such region. The presence of such a source region appears to result in a relative amplification of the high frequen-

20. DISTRIBUTION/AVAILABILITY OF ABSTRACT UNCLASSIFIED/UNLIMITED ☒ SAME AS RPT. ☐ DTIC USERS ☐	21. ABSTRACT SECURITY CLASSIFICATION UNCLASSIFIED
22a. NAME OF RESPONSIBLE INDIVIDUAL James Lewkowicz	22b. TELEPHONE NUMBER (Include Area Code) (617) 377-3028 22c. OFFICE SYMBOL AFGL/LWH

DD FORM 1473, 83 APR EDITION OF 1 JAN 73 IS OBSOLETE

UNCLASSIFIED

SECURITY CLASSIFICATION OF THIS PAGE

cy part (200-400 KHz) of the signal. If we scale the results so that they correspond to a cylindrical basin roughly the size of Yucca Flat, this means that frequencies analogous to 3-10 s in the Earth appear to be amplified relative to lower frequencies. When the source is excited in the graben in an off-center position, a radiation pattern is established, with amplitude varying by a factor of 2 or more. Material effects appear to be accentuated when the source is excited off-center.

Experiments on the scale model of Yucca Flat yield, in general, less dramatic results. The loss of symmetry apparently leads to less opportunity for focussing, and amplifications are not as great. Waveforms do not vary as much azimuthally in character or shape as they do in the cylindrical case, nor do they vary as much with source position within the graben. The most dramatically different waveforms are obtained when the source is excited over the deepest portion, in the southern part of the structure. This is outside the area corresponding to the portion of the basin where most explosions have been detonated. The effect is also enhanced for wave propagation directions to the northwest or southeast. Although effects are not as dramatic as they are in the case of the cylindrical graben, there is still a relative amplification of what corresponds to waves of period 2 s or shorter in the Earth, caused by the presence of the structure.

In the real Earth, Yucca Flat is not embedded in a homogeneous half space, but in a more complex multilayered structure, this possibly having a significant effect on seismic waveforms. It would be beneficial to conduct experiments involving grabens embedded in multilayered structures, and themselves filled with a multilayered material.

TABLE OF CONTENTS

LIST OF FIGURES

LIST OF FIGURES

LIST OF FIGURES

1. Introduction

The overall purpose of the Ultrasonic Physical Modeling Program at the Rockwell International Science Center is to model seismic wave propagation in the Earth using ultrasonic wave propagation in scale laboratory models. By using well-calibrated sources and receivers, our hope is to shed light on the effects of complex structure and geology on the propagation of seismic waves, and thus aid the national research effort in seismic monitoring of nuclear explosions. The intent is to complement numerical modeling, providing insight and guidance in complex situations where such modeling may not yet be feasible, owing to limitations in computer power.

In this report, we address the general problem of a nuclear explosion source region which has material properties significantly different from those of the surrounding seismic wave propagation medium. Such a situation exists, for example, in the case of explosions set off in Yucca Flat at the Nevada Test Site. The existence of a source region with differing material properties from the surrounding medium can have considerable effects on recorded surface wave amplitudes, as has been shown by some numerical studies (e.g., Regan and Glover, 1985). This in turn has implications for yield estimation, and possibly for discrimination.

2. The Receiver

It is absolutely imperative in a study of this kind to have a receiver with a well-known response. We use an NBS-type conical transducer (Proctor 1980, 1982a,b) manufactured by Industrial Quality, Inc.; it is shown in Fig. 1. This transducer is a vertical component displacement sensor with a 1 mm contact area, and a very flat response. The element is piezoceramic, and it is coupled to a large brass backing which effectively eliminates resonances, as well as minimizing coherent reflections back into the element. Figure 2 shows typical response curves for this type of transducer, sent to us by NBS. The response is flat enough that when we look at a signal from this transducer, we can consider that we are looking essentially at raw vertical component displacement.

SC37734

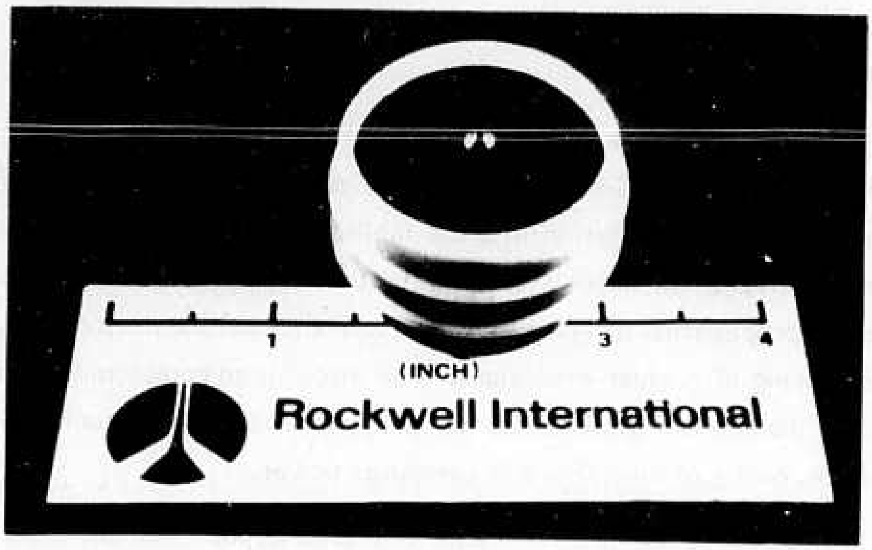

Fig. 1 The NBS-type conical transducer used in this study, showing the point-like probe.

3. The Source

Just as important as having a well-characterized receiver is having a well characterized source. The source we use is a simple one, but it is quite effective. Basically, we achieve a step-function point unloading of the surface by breaking a pencil lead on it. This is a variant of the well-known breaking-glass-capillary source used by the NBS, and is discussed in detail by Hsu and Hardy (1978). Figure 3 shows a picture of the source assembly, and Fig. 4 shows the source time function of the breaking pencil lead, obtained via deconvolution by Hsu and Hardy. The apparent noisiness in the response is due to the deconvolution process. The source approximates a step function; actually it is a ramp, but the rise time of the ramp is less than 1 μs.

4. Lamb's Problem

Figure 5 shows the result of a measurement made by setting off the source on the gabbro "halfspace", and recording the signal received by the transducer 200 mm away

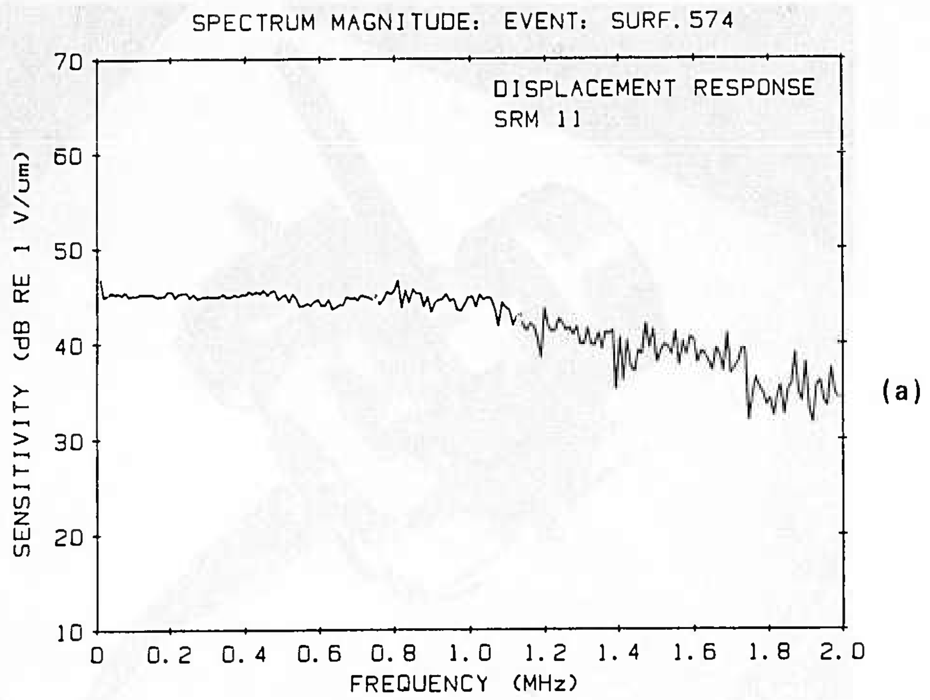

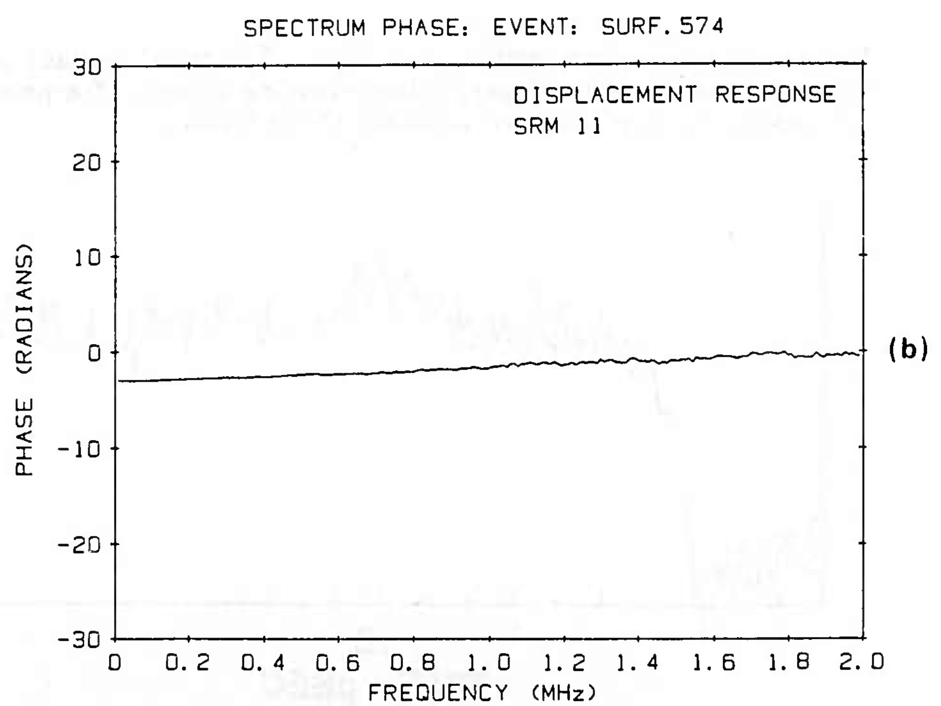

Fig. 2 Typical displacement response curves for the NBS-type conical transducer. a) Amplitude. (b) Phase. The receiver is close to a true displacement sensor.

SC37733

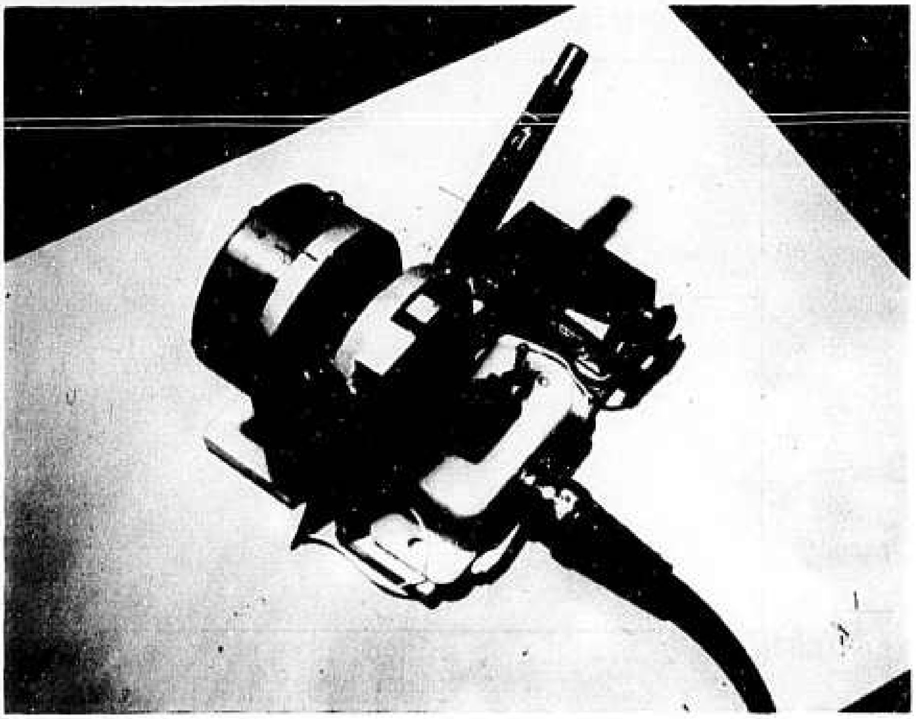

Fig. 3 The pencil-lead source used in this study. Electrical contact is broken when the pencil lead breaks, triggering the recording system. The pencil-lead source corresponds to step function unloading of the surface.

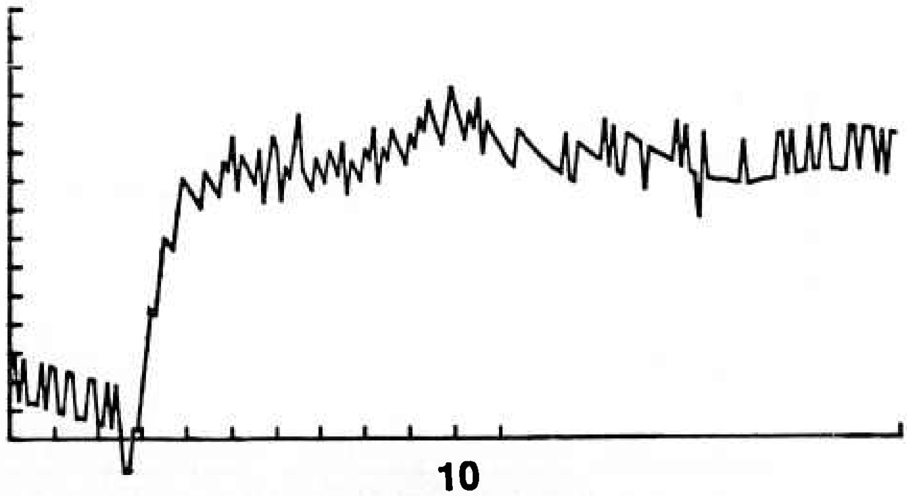

Fig. 4 Source-time function of a pencil lead source, obtained by Hsu and Hardy (1978) by deconvolution. Some spurious structure has been introduced by the deconvolution.

(the standard distance for all the measurements presented in this report). The displacement record is essentially a solution of the classic Lamb's problem (see e.g., Miklowitz, 1978; Mooney, 1974; Breckenridge et al, 1975) for a point force on a surface. Figure 5 shows, for comparison, the result of Boler et al, (1984) for a similar setup, using a breaking-glass-capillary source and a true displacement transducer. The results are very similar in appearance to ours. Boler et al include the theoretical response computed from Lamb's solution. The first arrival P wave is very small in the theoretical solution, and is very small in Boler et al's measurements. In our results, there is only a hint of it, as a minor inflection before the onset of the large signal. The large signal observed in both our record and in Boler et al's is, of course, the S wave followed by the Rayleigh wave.

5. The Cylindrical Graben Model

As a first step towards studying this problem, we have studied a cylindrical low velocity "graben," or plug, embedded in a high velocity medium (Fig. 6). The high velocity medium is a fine-grained gabbro with V_p = 6.2 km/s, V_s = 3.6 km/s, and V_R = 3.3 km/s. The plug is filled with lower velocity materials, whose properties are shown in Table 1.

Table 1
Properties of Modeling Materials

Material	Longitudinal Velocity V_p, km/s	Shear Velocity V_s, km/s	Rayleigh Velocity V_R, km/s	Poisson's Ratio ν	Density ρ, g/cc
Crystalbond 504 (Aremco Prods. Inc.)	2.407	1.096	1.01	0.369	1.32
HPAL3	3.287	1.742	1.61	0.305	2.01
Gabbro	6.200	3.623	3.33	0.240	2.97

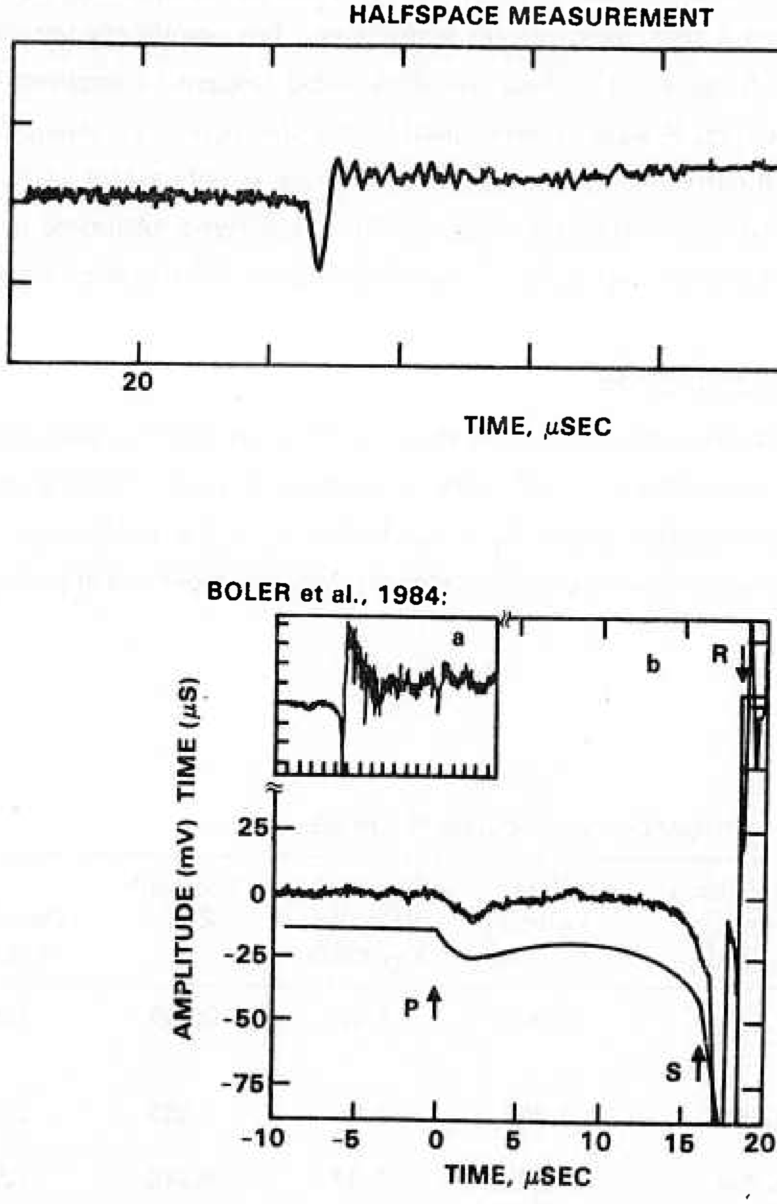

Fig. 5 Signal observed by actuating the source on the gabbro "halfspace." Similar signals obtained by Boler et al (1984) are shown for comparison.

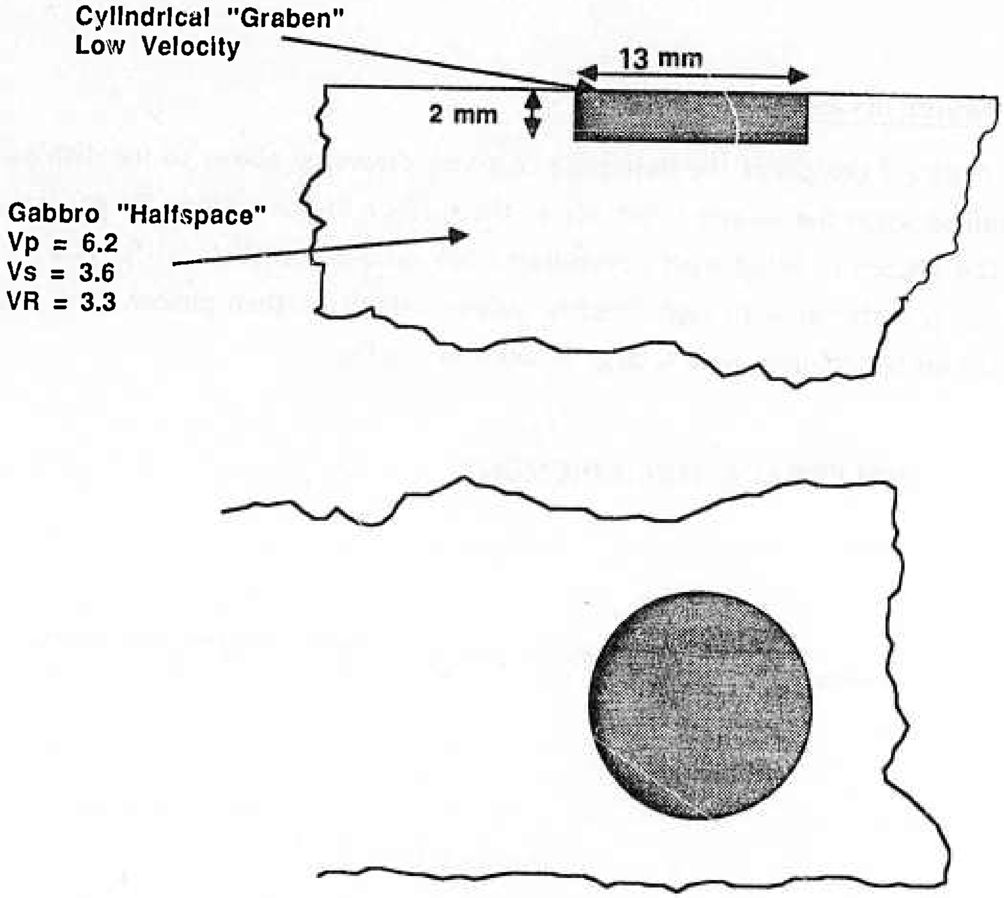

Fig. 6 The model of a cylindrical graben filled with low velocity material, embedded in a fine-grained gabbro "halfspace."

It is important to have a good idea of the scale factors involved. Taking Yucca Flat as a rough guideline, we may say that a graben of interest in the Earth is roughly $L^e = 20$ km in diameter. If the source material in the Earth has a Rayleigh wave velocity $V_R{}^e = 1.2$ km/s, then a 20 s Rayleigh wave in the Earth has a wavelength $\lambda_R{}^e = 24$ km $\approx L^e$. Now, the model graben has a diameter L^m of 13 mm. We would like to know the frequency in the model of the Rayleigh wave analogous to a 20 s Rayleigh wave in the Earth. The wavelength of this analogous wave in the model graben must be roughly equal to the graben diameter, i.e., $\lambda_R{}^m \approx L^m$. Since $V_R{}^m$ ranges from roughly 1 to 1.6 km/s, this means that the frequency ranges from roughly 80 to 120 kHz, depending on the material in the graben. Hence, Rayleigh waves of 80 to 120 kHz in the model are analogous to 20 s Rayleigh waves in the Earth.

5.1 Source in Graben, Centered

Figure 7 compares the halfspace response discussed above to the displacement signal obtained when the source is set off at the surface of the cylindrical graben, in the center. The graben is filled with Crystalbond 504 (also referred to as "crystal wax" in the figures), a material with significantly slower velocities than gabbro (see Table 1). The signal is quite complex, with a large amount of ringing.

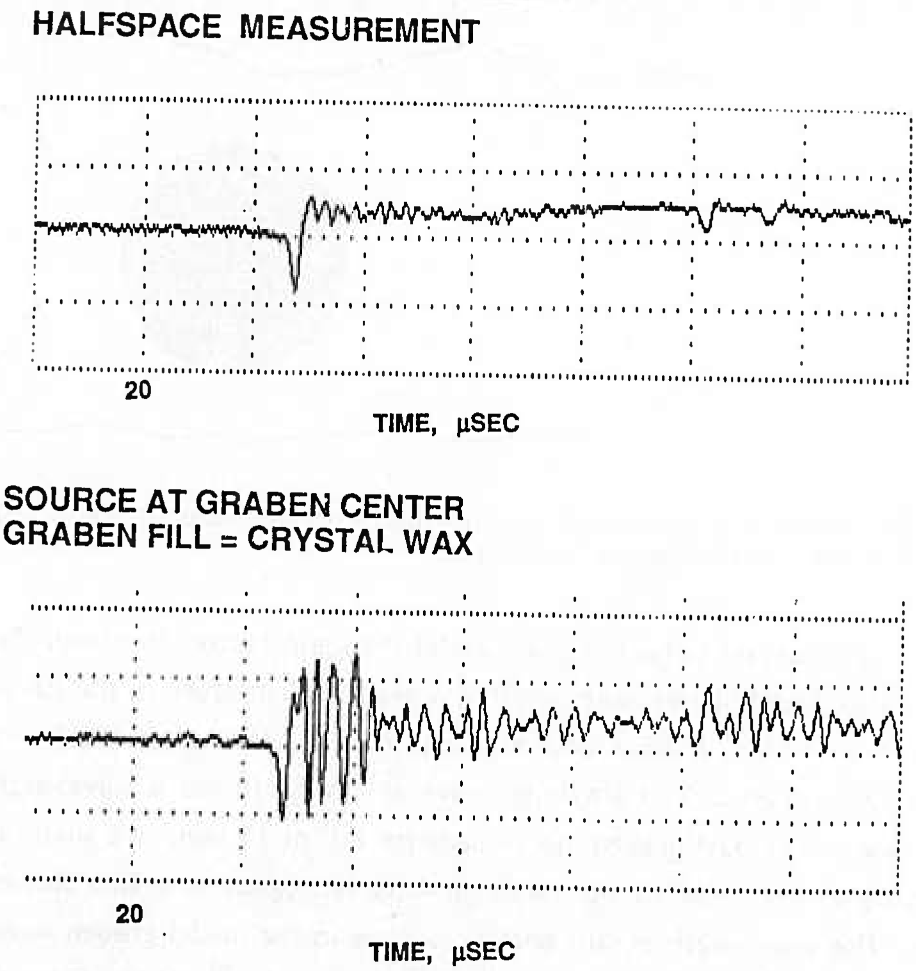

Fig. 7 Comparing the halfspace signal (also shown in Fig. 5), with the signal observed when the source is actuated at the center of the surface of the cylindrical plug ("graben") filled with Crystalbond 504. Source-receiver distance is 200 mm. Vertical scale is 100 mV per division.

Energy which, when the source is set off on the halfspace, goes downward and is not recorded at the surface, is now trapped and redirected by the graben structure.

Figure 8 compares the results from a centered source in the graben for two different fill materials. The top trace is a copy of the signal discussed immediately above, where the graben is filled with Crystalbond 504. The bottom trace is for a graben filled with HPAL3, an aluminum-filled resin with faster velocities than Crystalbond 504, but slower velocities than gabbro. As might be expected, the amplitude of the ringing is smaller than in the case of Crystalbond 504. As the material property contrast increases between the graben and the surrounding medium, the observable effects of ringing appear to increase.

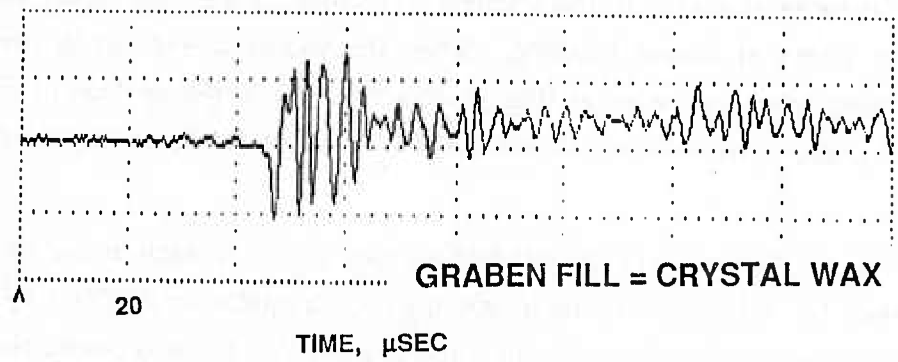

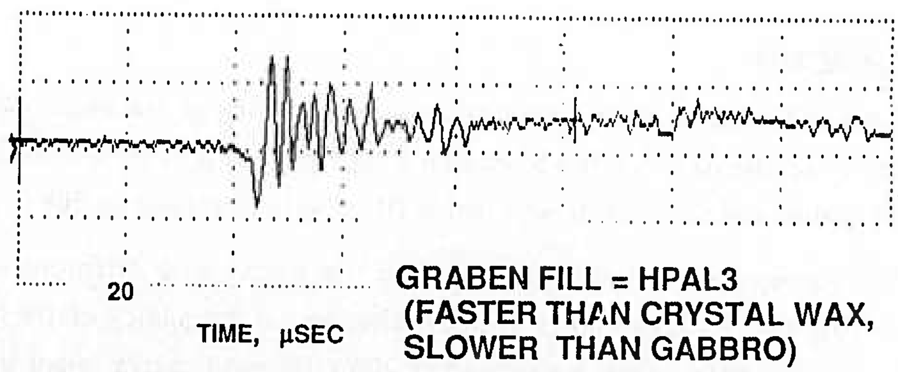

Fig. 8 Comparing signals from a source at the graben center. Top trace is for a graben filled with crystal wax (same as Fig. 7); bottom trace is for a graben filled with HPAL3. HPAL3 is faster than Crystalbond ("crystal wax"), but slower than gabbro. Source-receiver distance is 200 mm. Vertical scale is 100 mV per division.

5.2 Source in Graben, Off-Center

Figure 9 shows signals obtained when the source is actuated in the graben in various off-center positions. The relative position of source and receiver is shown schematically in plan view beside each trace. In each case, the source is actuated along a diameter, halfway between the center and the rim of the graben. (It is easy to see that this is as if the source were kept in one of the three positions, and the receiver were moved around.) Clearly, an off-center source produces a radiation pattern. Both the shape and amplitude of the signal depend on the relative position of source and receiver. The trace with the largest amplitude has a maximum peak-to-peak amplitude about twice as large as that with the smallest amplitude. These results are fairly easy to rationalize in terms of simple focusing. When the source is excited in the off-center position furthest from the receiver (Fig. 9, top trace), a larger portion of the boundary between the graben and the rest of the medium is illuminated in the direction of the receiver.

Figures 10 through 12 show the off-center signals in each of the three positions just discussed, for different fill materials (again, Crystalbond 504 and HPAL3). The effect on amplitude of the different fill materials appears to be accentuated in the off-center cases.

5.3 Voiceprints

Figures 13 and 14 show an interesting presentation of the data. What is shown is a "voiceprint" of the data for the source on a halfspace (Fig. 13), and the data for the source in the graben center when the graben is filled with Crystalbond 504 (Fig. 14).

The voiceprint is obtained by filtering the traces with different bandpass filters, and plotting the results in order of increasing center frequency of the bandpass filter. In this case, the filters have a passband of 200 kHz, and the increment in center frequency between traces is 40 kHz. Thus, the bottom trace shows the data filtered from 0-200 kHz (center frequency 100 kHz), the next trace up shows the data filtered from 40-240 kHz (center frequency 140 kHz), the next trace after that shows the data filtered from 80-280 kHz (center frequency 180 kHz), etc. What results is essentially a frequency-time plot. (Note that the traces are also rectified and low pass filtered, to avoid spurious wiggles resulting from the increasing center frequency of the bandpass filter.)

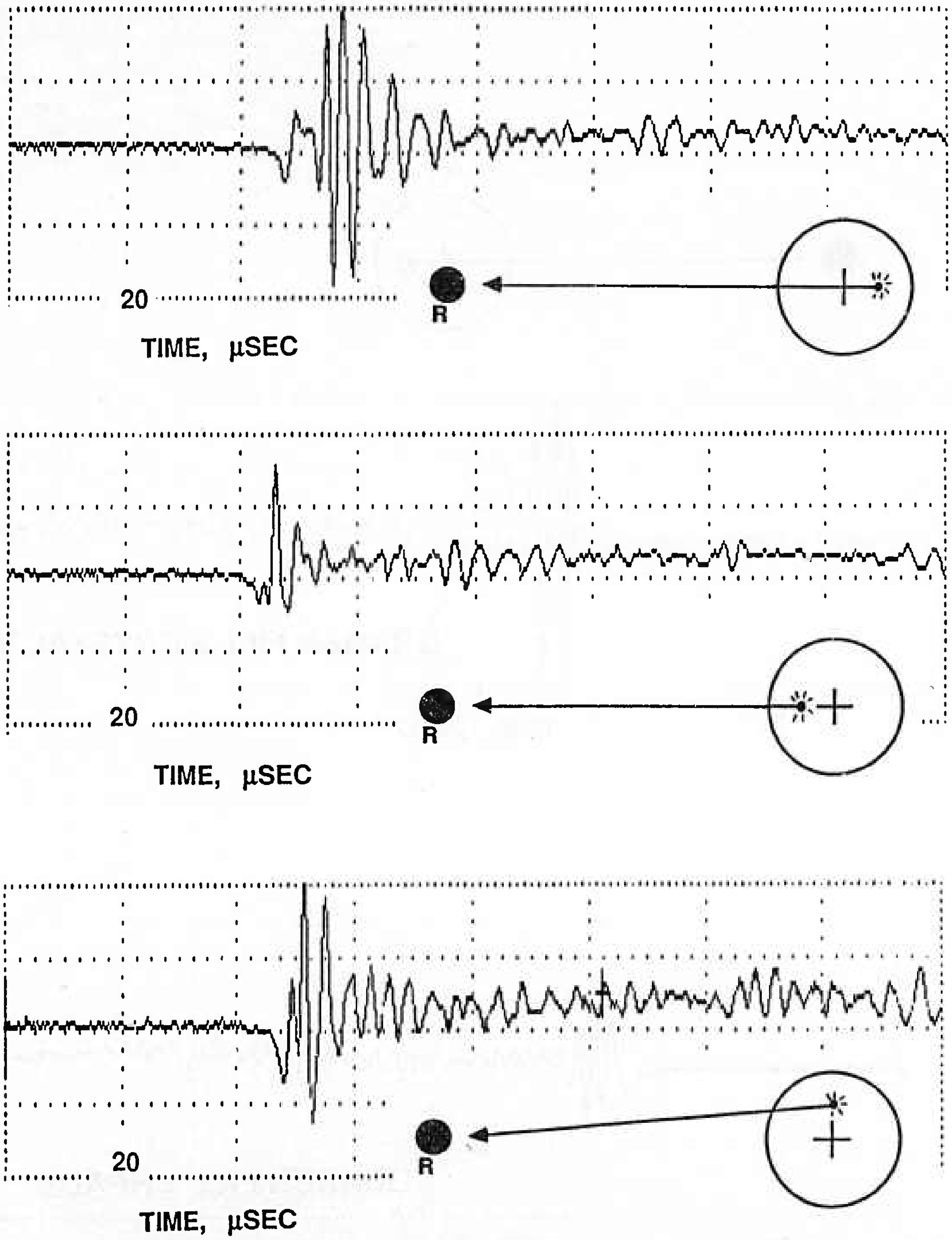

Fig. 9 Signals from sources actuated off-center in a graben filled with Crystalbond 504 ("crystal wax"). Each trace is accompanied by a plan view showing the relative positions of source and receiver. Distance from graben center to receiver is 200 mm. Vertical scale is 200 mV per division for the two top traces, and 100 mV per division for the bottom trace.

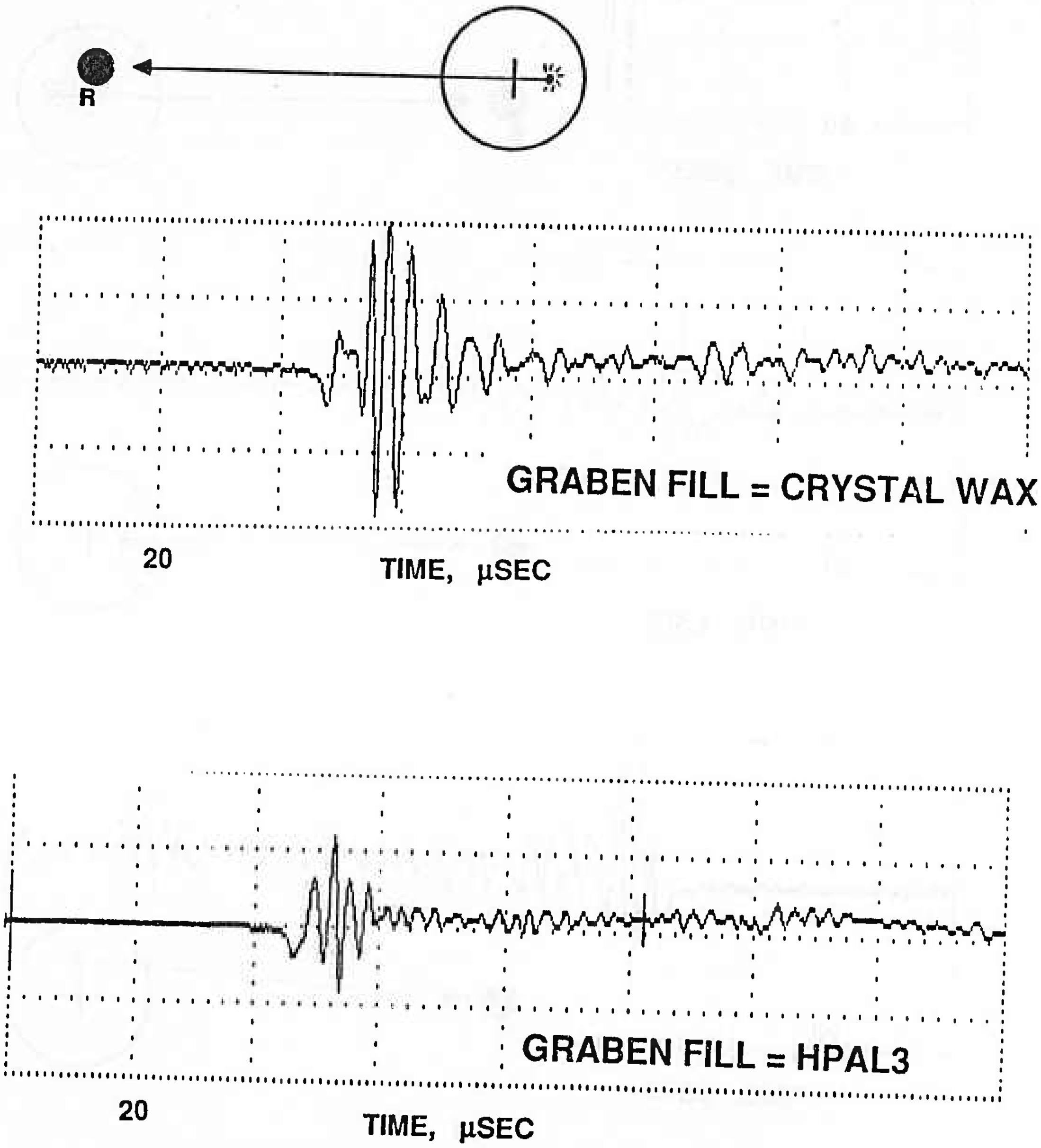

Fig. 10 Signals for one of the off-center positions in Fig. 9, for a graben filled with Crystalbond 504 ("crystal wax") and a graben filled with HPAL3. Distance from graben center to receiver is 200 mm. Vertical scale is 200 mV per division.

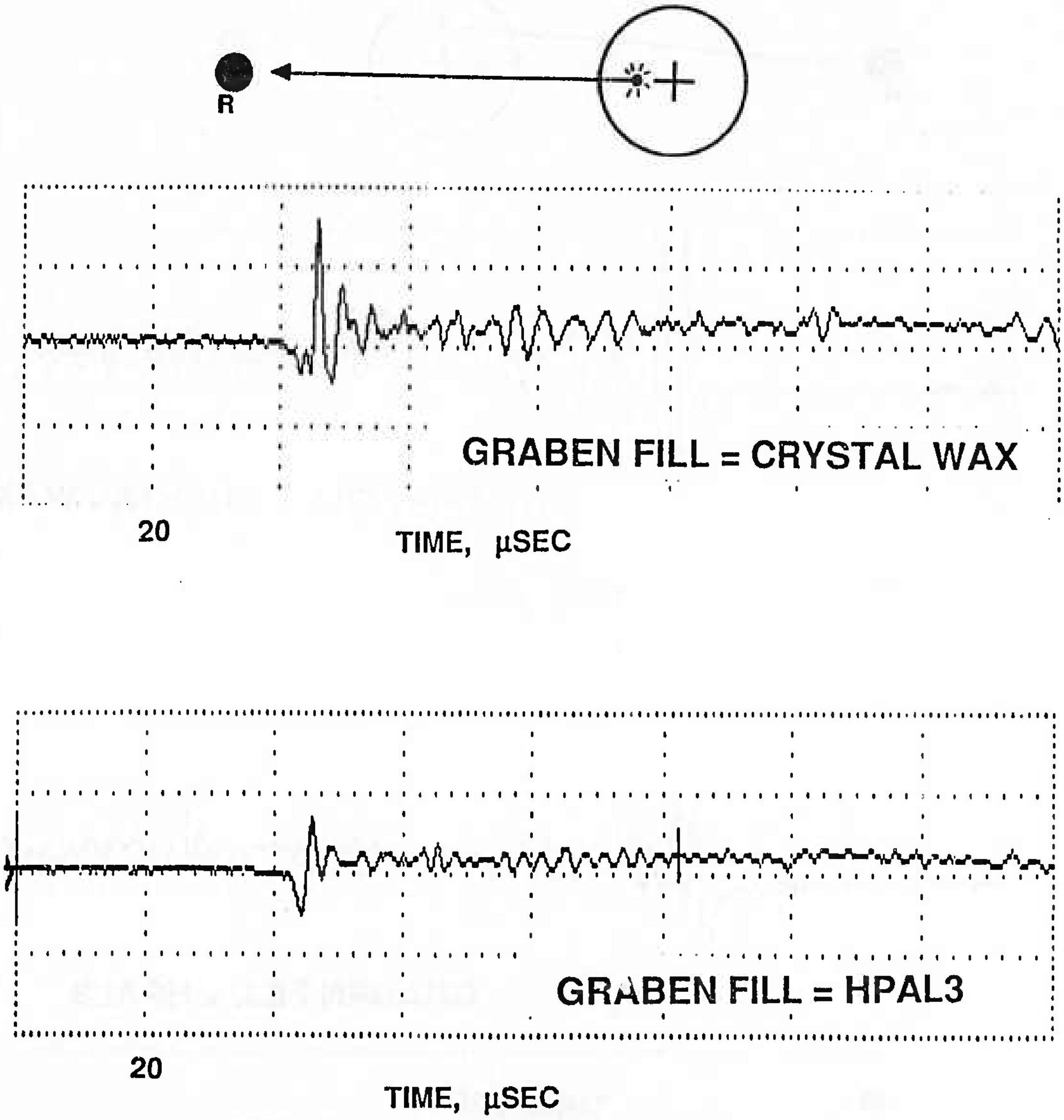

Fig. 11 Signals for one of the off-center positions in Fig. 9, for a graben filled with Crystalbond 504 ("crystal wax") and a graben filled with HPAL3. Distance from graben center to receiver is 200 mm. Vertical scale is 200 mV per division.

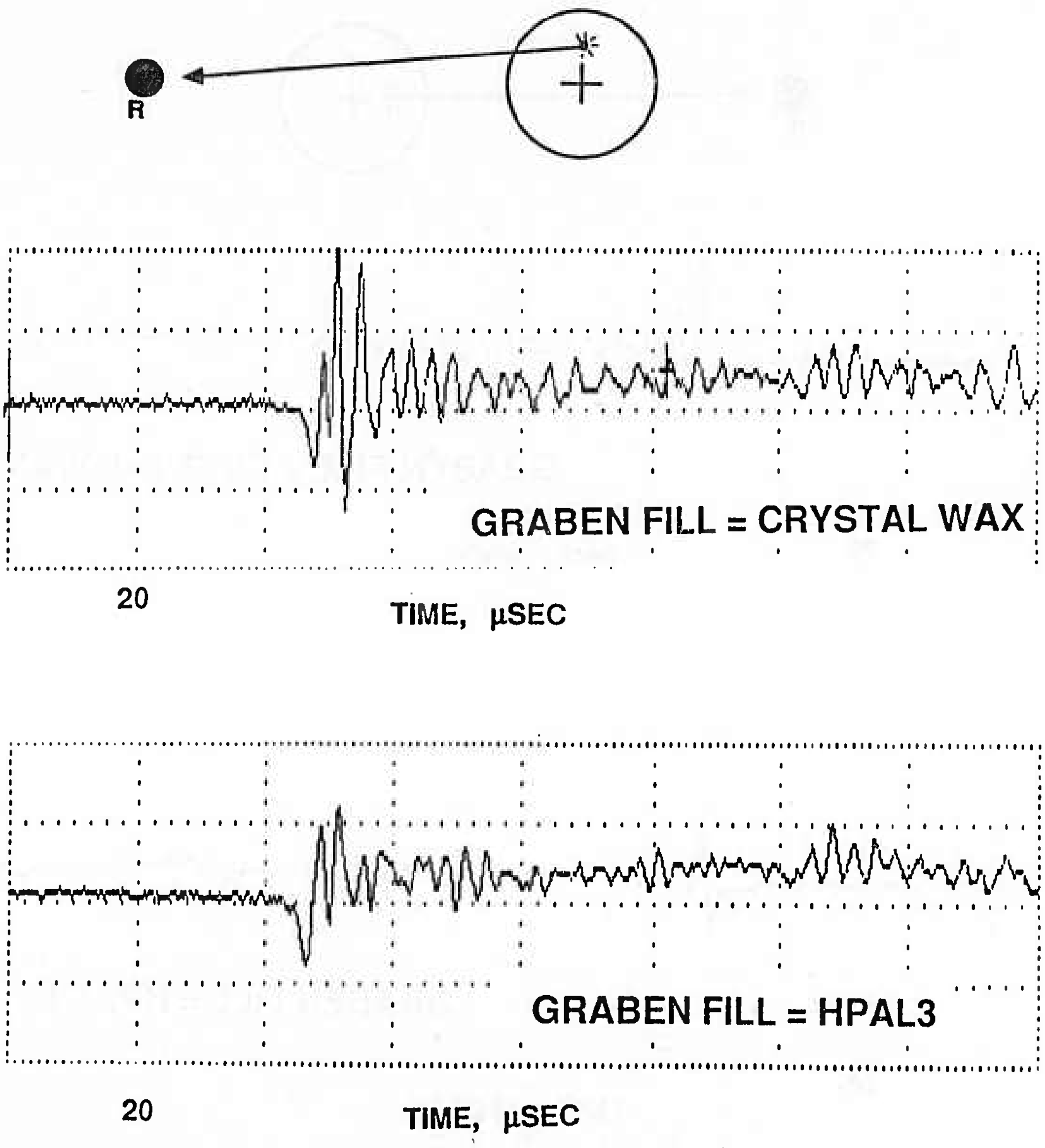

Fig. 12 Signals for one of the off-center positions in Fig. 9, for a graben filled with Crystalbond 504 ("crystal wax") and a graben filled with HPAL3. Distance from graben center to receiver is 200 mm. Vertical scale is 100 mV per division.

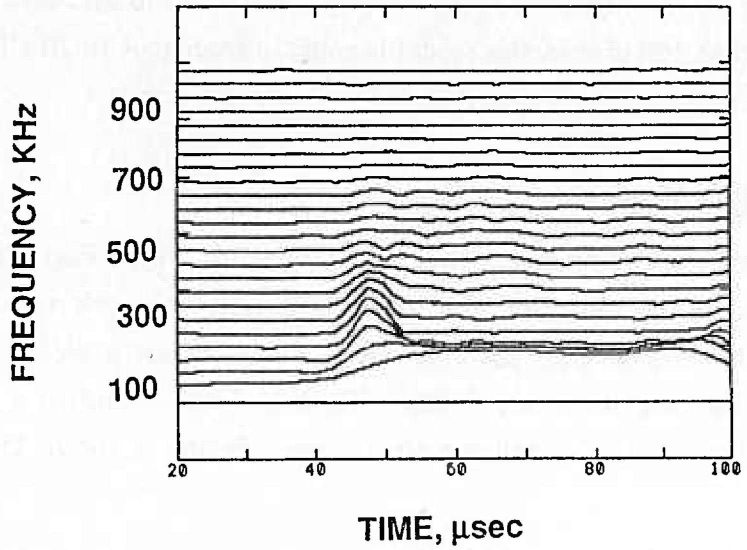

Fig. 13 "Voiceprint" of the halfspace signal shown in Fig. 6. Each trace in the voiceprint represents the signal filtered by a bandpass filter with a bandwidth of 200 kHz. The increment in center frequency of the filter is 40 kHz as we move from the bottom trace upwards. Thus, this is a time-frequency diagram.

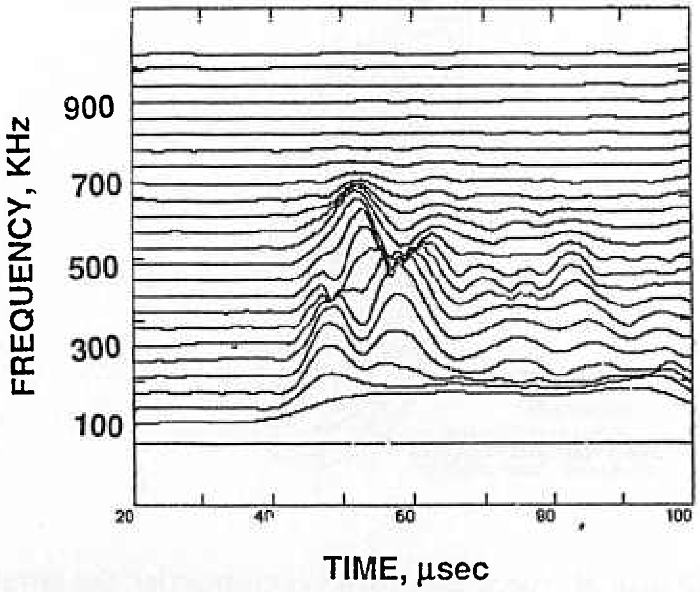

Fig. 14 Voiceprint similar to that in Fig. 13, but this time for the signal of Fig. 7, the signal from the source actuated in the graben center when the graben is filled with Crystalbond 504 ("crystal wax").

Examination of the voiceprints shows that although the low-frequency levels are quite similar between the two cases, the case with the source in the graben has considerably more energy in the higher frequency range, from 500 to 700 kHz center frequency. Considering that 100 kHz in the model is roughly analogous to 20 s in the Earth, this 500 to 700 kHz range corresponds roughly to 3 or 4 s in the Earth.

6. The Yucca Flat Model

We have constructed an accurate scale model of Yucca Flat, based on the generalized map shown in Fig. 15, which was constructed from the work of Ferguson et al (1986). The rectangular box outlines an area where many nuclear explosions have been detonated (see, e.g., McLaughlin et al, 1986). The basin was drilled in a fine-grained gabbro halfspace and filled with Crystalbond 504 (Aremco Products, Inc.). The properties

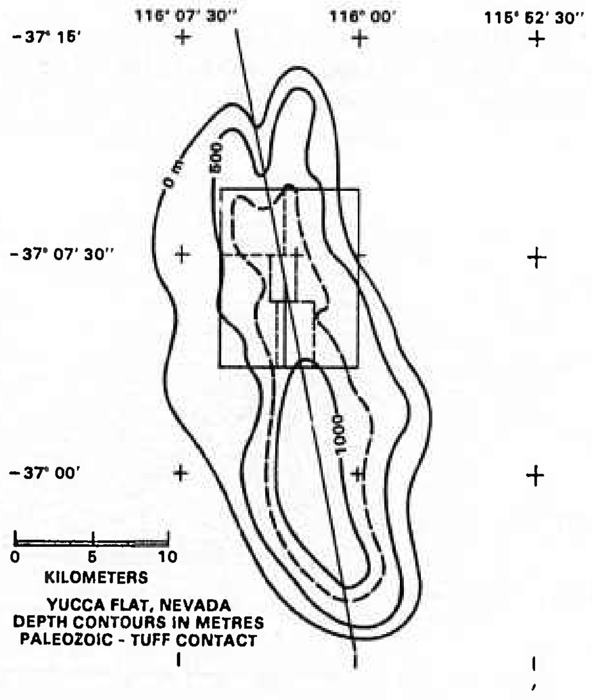

Fig. 15 Generalized map of Yucca Flat used in constructing the physical model. Map was drawn based on the work of Furgeson et al (1986). Large rectangle delineates area where many explosions were located.

of the gabbro and Crystalbond are given in Table 1. The source is excited on the surface of the basin and receivers are placed outside the basin on the halfspace, as shown in Fig. 16.

1 mm in the model represents 1 km in the Earth. If the material filling the basin in the Earth has a Rayleigh wave velocity V_R = 1.2 km/s, then a 20 s Rayleigh wave in the Earth has a wavelength of 24 km. Thus, the analog of the Earth's 20 s Rayleigh wave has a wavelength of 24 mm. Given that the basin fill material has a Rayleigh wave velocity of 1.01 km/s, this corresponds to a frequency of about 40 kHz. Thus, in this scale model of Yucca Flat, a 40 kHz Rayleigh wave corresponds ***roughly*** to 20 s Rayleigh wave in the Earth.

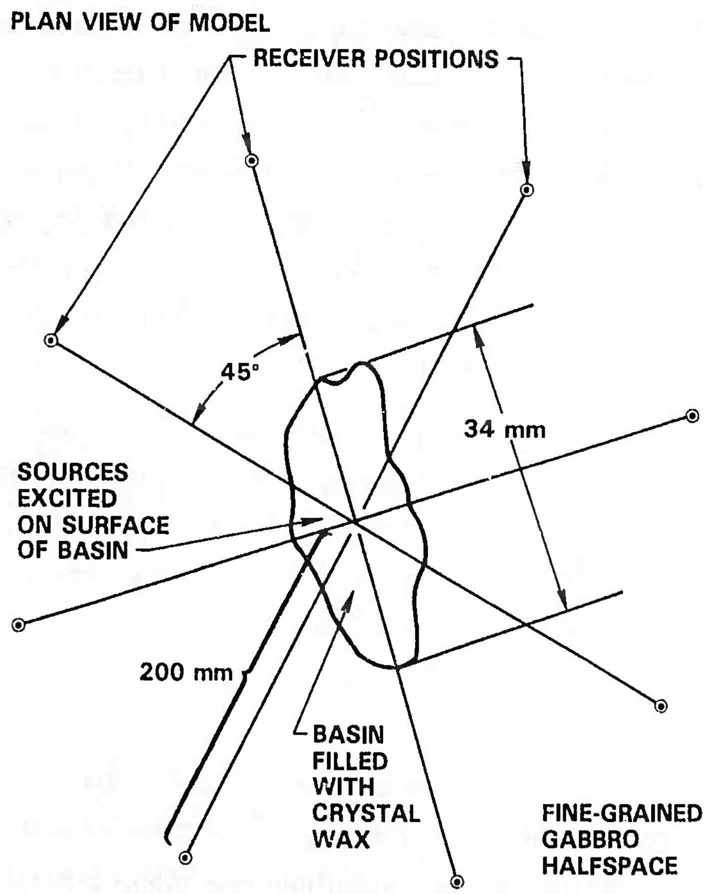

Fig. 16 Overall geometry of the model. "Crystal wax" refers to Crystalbond 504 (Aremco Prods., Inc.)

6.1 Source Excited Within the Scale Model of Yucca Flat

Figures 18-21 show the waveforms obtained when the source was excited on the surface of the basin. For comparison, Fig. 17 shows the waveforms obtained when the source was excited in the gabbro before the basin was excavated. In each case, the receiver positions are identical - 200 mm from the same reference point in the basin (the same point as the source position in Fig. 20).

The figures are meant primarily to illustrate waveform character; they should not be used as an accurate guide to arrival times. Arrival times are not completely reliable because of triggering problems in the apparatus, which we have subsequently rectified.

Examination of Figs. 18-21 yields the perhaps rather surprising result that the presence of the basin does not seem to be making much difference in the shape of the waveform. When the source is anywhere within the rectangular box representing the location of many actual explosions (Figs. 18-20), the waveforms appear almost like half-space responses. There does appear to be some complexity and ringing, but nothing like what is observed in the case of the cylindrical plug graben. The loss of symmetry in going from a cylindrical plug graben to a more realistic structure seems to have dramatically reduced the focusing effects.

The only case where relatively dramatic effects on the waveshapes is observed is shown in Fig. 21, when the source is excited over the deepest portion of the graben. Here, we see some of the same kind of complexity and ringing observed in the cylindrical plug graben. This is not difficult to rationalize, because the structure at this position locally approximates a plug or bowl-like structure.

6.2 Spectral Ratios

Figures 22 and 23 show some spectral ratios for the data in Figs. 19 and 21. At each position, the magnitude spectrum of the waveform obtained with the source excited on the basin surface is divided by the magnitude spectrum of the waveform obtained through the gabbro before the basin was excavated. If the spectral value of the denominator is too small (5% or less of its maximum value), the ratio is set to zero. Thus, we obtain some notion of the effect of the structure on the wave propagation.

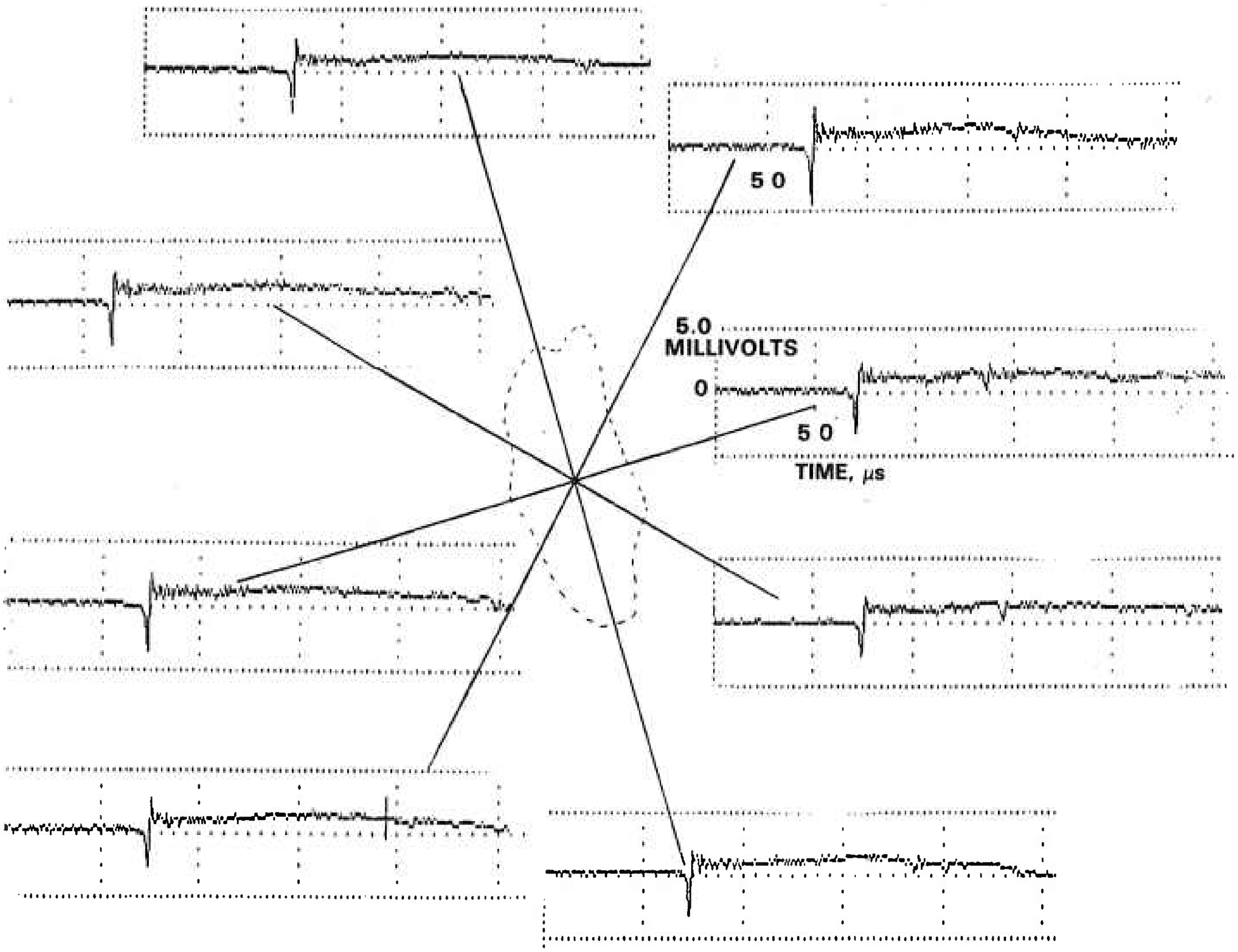

Fig. 17 Waveforms obtained on the gabbro halfspace before the Yucca Flat model was excavated. Vertical scale is 50 mV per division. Horizontal scale is 50 μs per division.

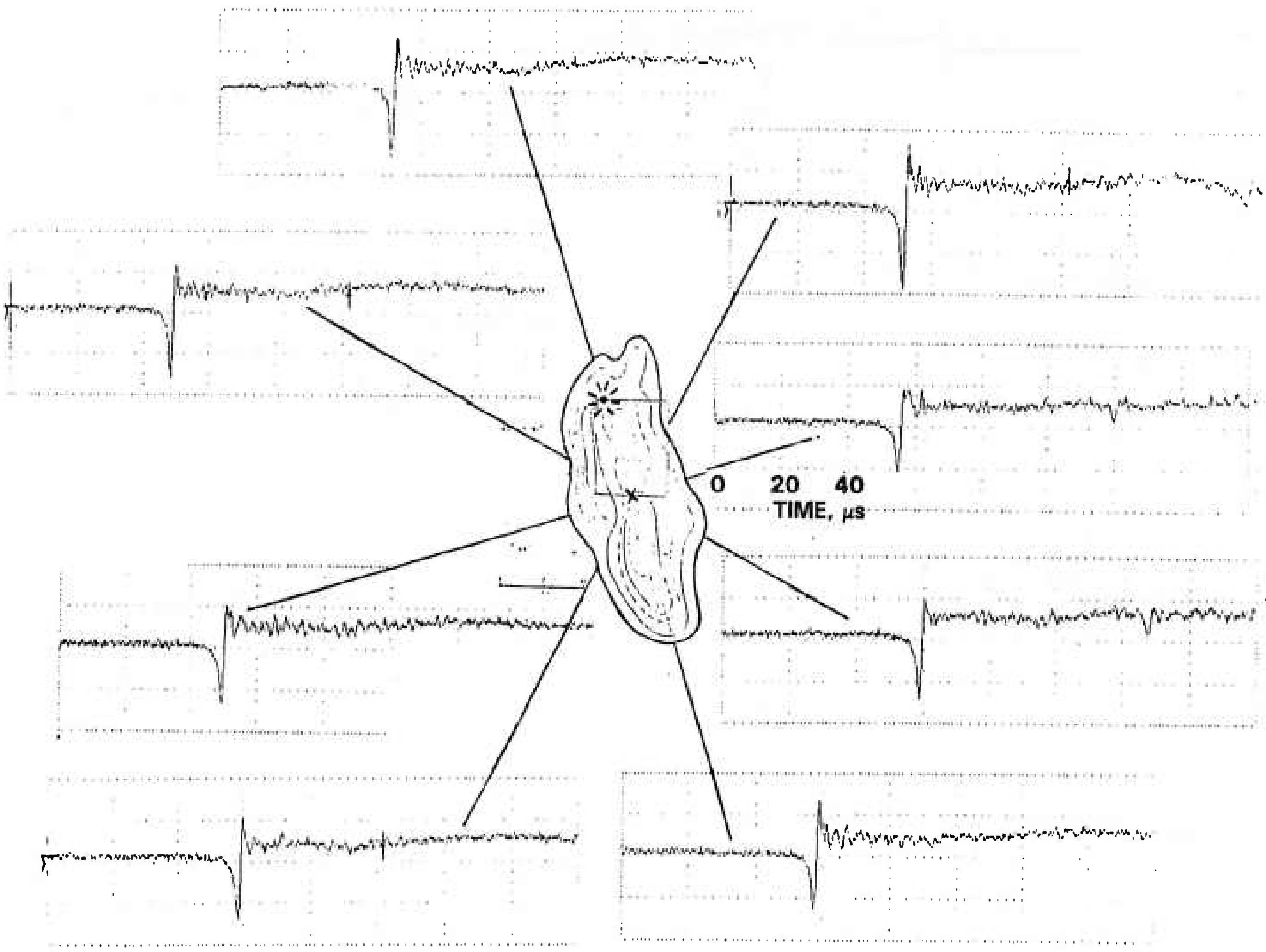

Fig. 18 Waveforms obtained from sources excited on the surface of the basin. The point "X" in each case is the reference point - all receivers are 200 mm from this reference point. The dot with the rays coming out of it indicates the position of the source in each case. In each case, the vertical scale is 20 mV per division, and the horizontal scale is 20 µs per division.

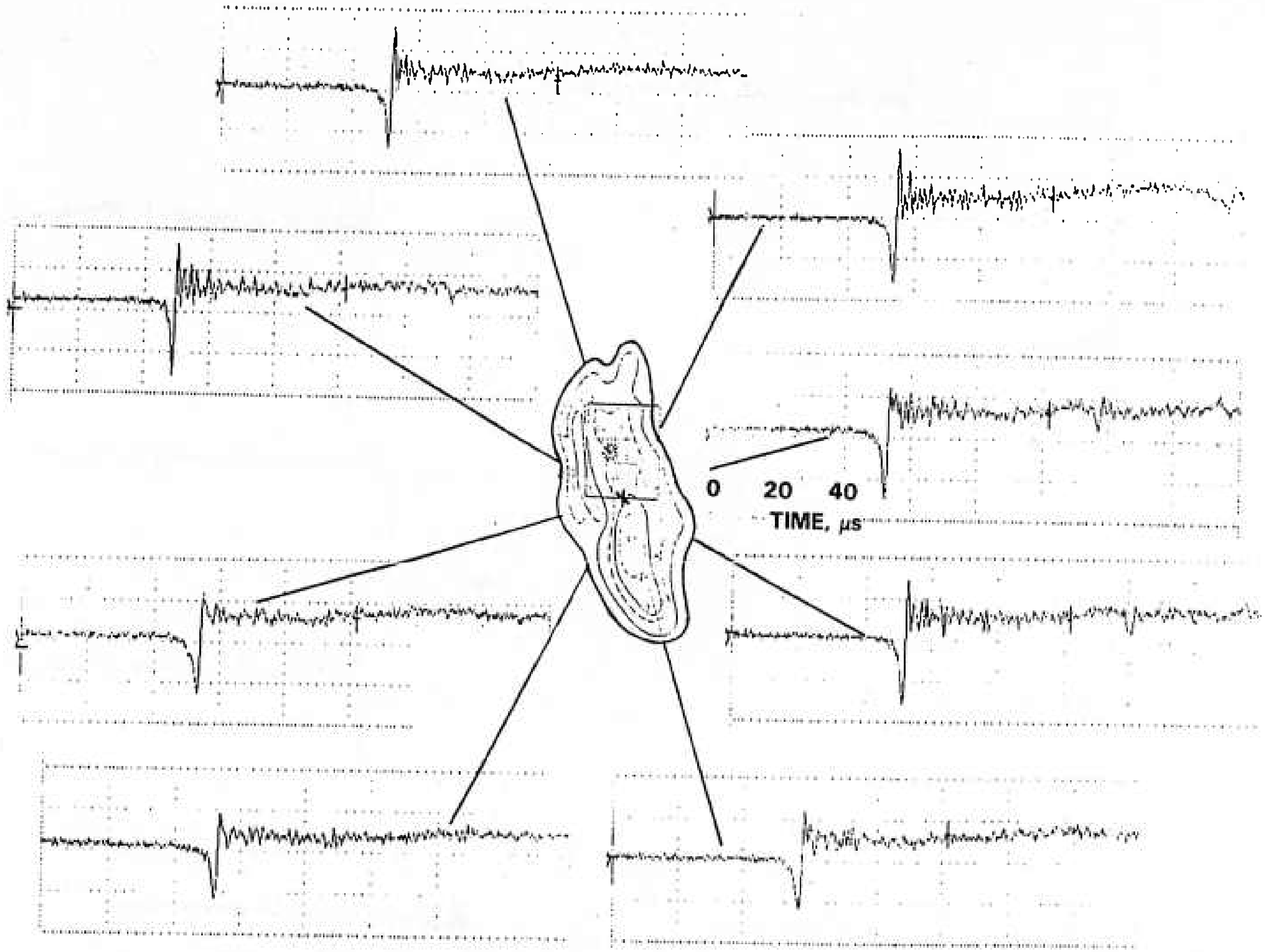

Fig. 19 Waveforms obtained from sources excited on the surface of the basin. The point "X" in each case is the reference point - all receivers are 200 mm from this reference point. The dot with the rays coming out of it indicates the position of the source in each case. In each case, the vertical scale is 20 mV per division, and the horizontal scale is 20 μs per division.

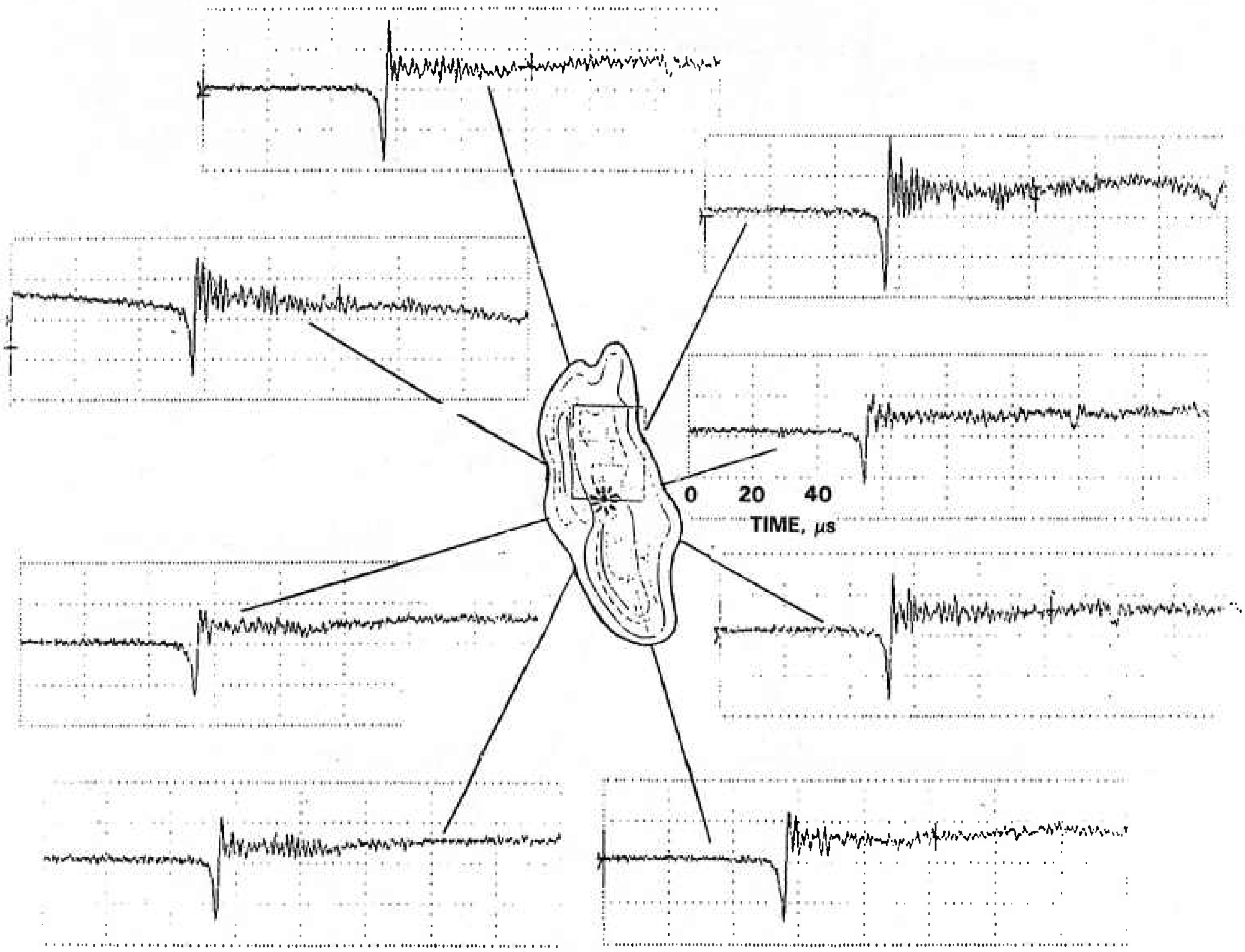

Fig. 20 Waveforms obtained from sources excited on the surface of the basin. The point "X" in each case is the reference point - all receivers are 200 mm from this reference point. The dot with the rays coming out of it indicates the position of the source in each case. In each case, the vertical scale is 20 mV per division, and the horizontal scale is 20 μs per division.

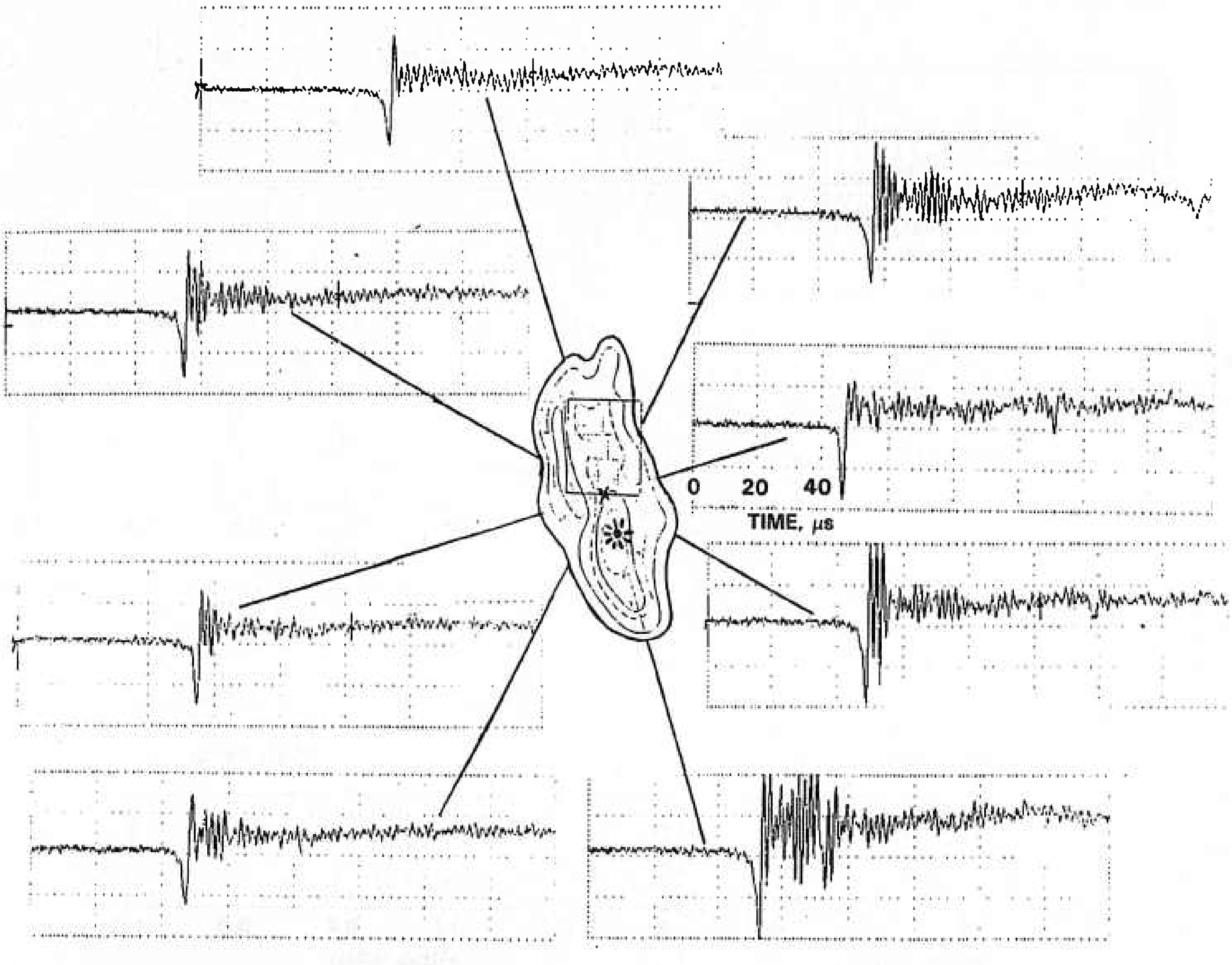

Fig. 21 Waveforms obtained from sources excited on the surface of the basin. The point "X" in each case is the reference point - all receivers are 200 mm from this reference point. The dot with the rays coming out of it indicates the position of the source in each case. In each case, the vertical scale is 20 mV per division, and the horizontal scale is 20 μs per division.

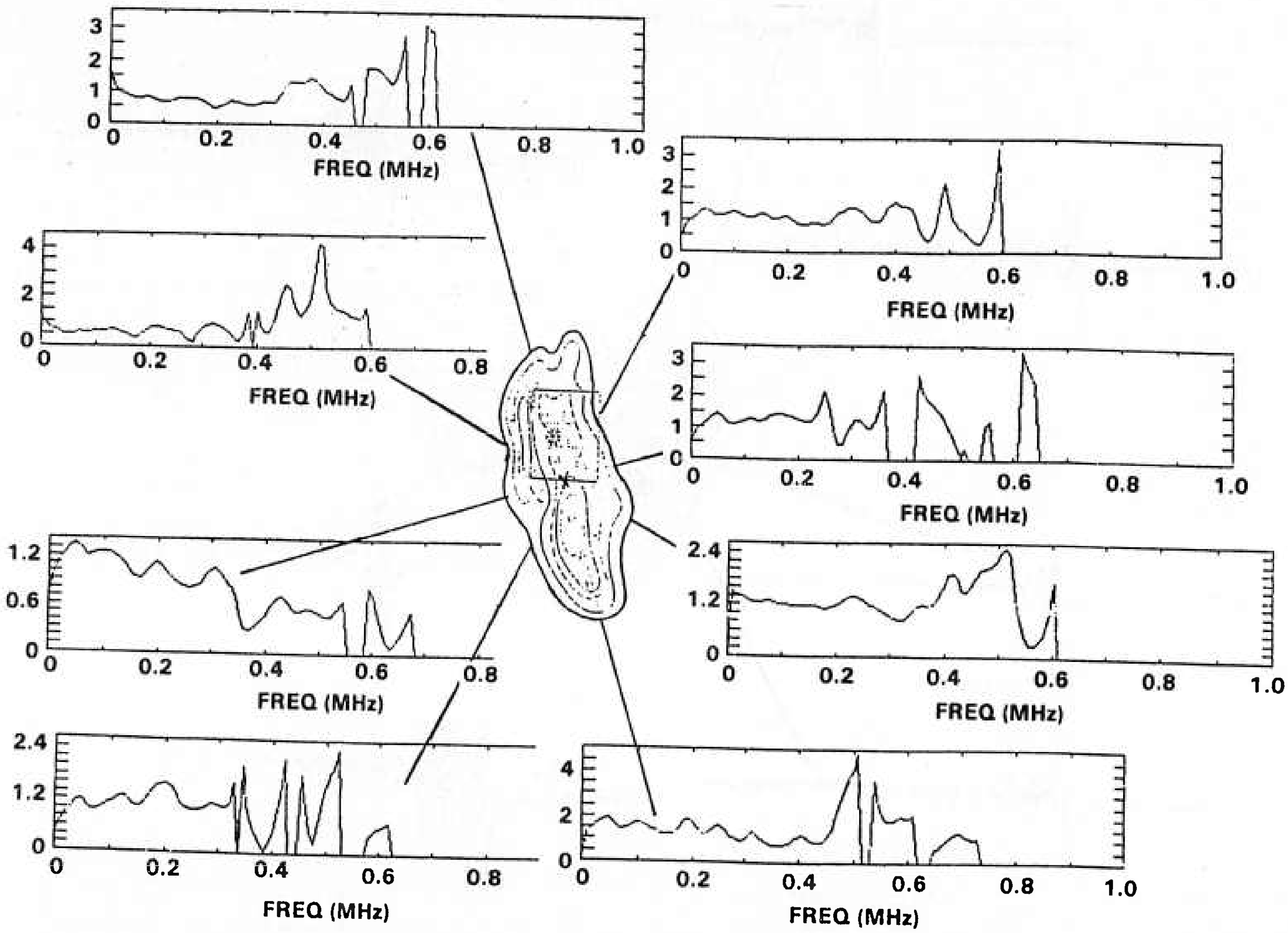

Fig. 22 Spectral ratios for the data in Fig. 19. At each position, the magnitude spectrum of the waveform obtained with the source excited on the basin surface is divided by the magnitude spectrum of the waveform obtained through the gabbro before the basin was excavated.

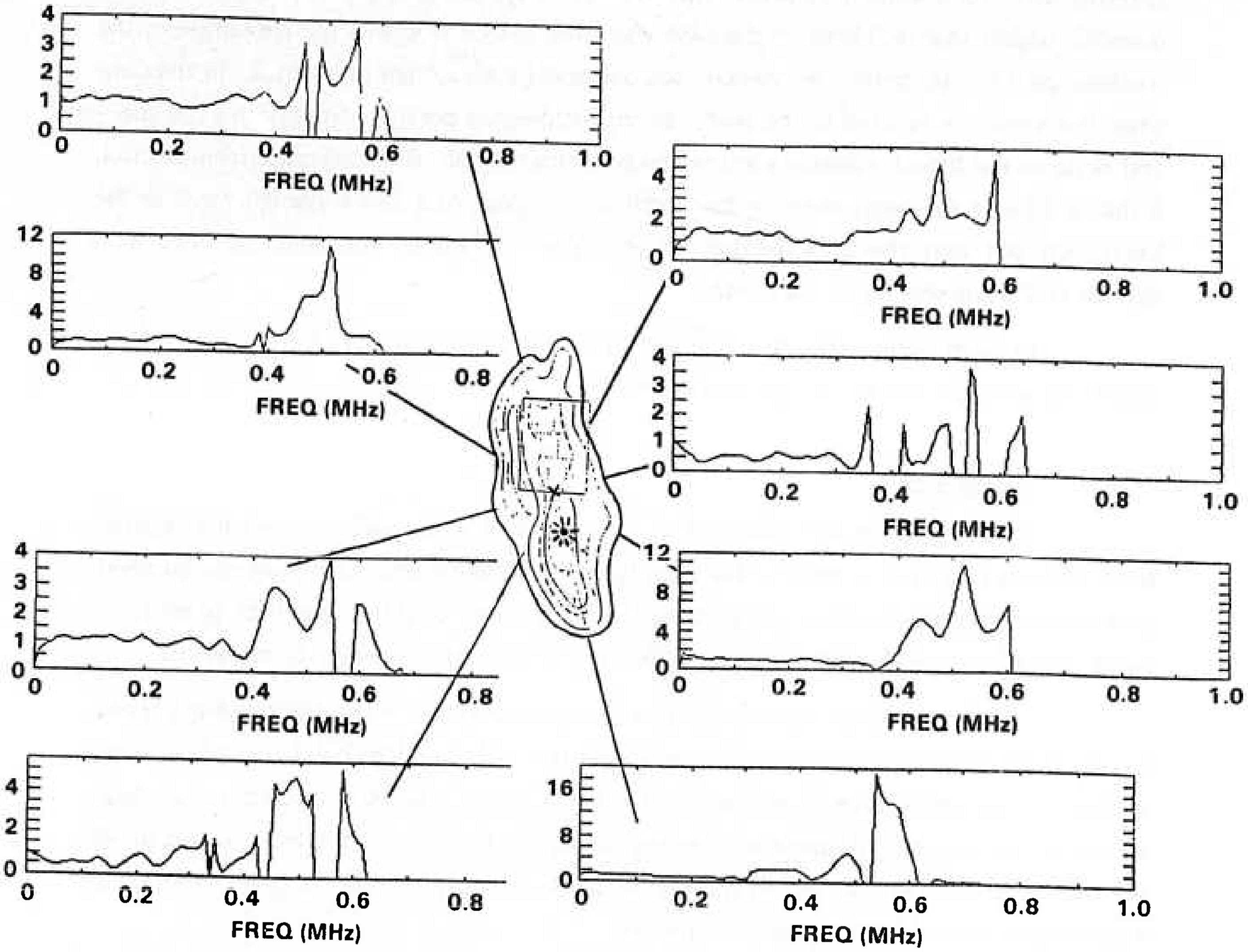

Fig. 23 Spectral ratios for the data in Fig. 21. At each position, the magnitude spectrum of the waveform obtained with the source excited on the basin surface is divided by the magnitude spectrum of the waveform obtained through the gabbro before the basin was excavated.

The spectral ratios indicate that the structure seems to be causing some amplification of high frequencies, above 400 kHz, relative to the lower frequencies. The spectral ratio for frequencies lower than 400 kHz is generally close to 1 or 2. For frequencies higher than 400 kHz, in the case when the source is within the rectangle in the northern part of the basin, the spectral ratio reaches a maximum of about 5. In the case when the source is located to the south, above the deepest portion of the basin, the spectral ratio in the high-frequency portion can be as high as 20. Remembering from Section 6 that a 40 kHz Rayleigh wave in the model is analogous to a 20 s Rayleigh wave in the Earth, we see that the amplification is occurring for waves analogous to ones with periods of 2 s and shorter in the Earth.

In both cases, the directions of greatest amplifications of high frequencies appear to lie in the southeast and the northwest.

7. Conclusions

We have described experiments intended to clarify seismic wave propagation from sources actuated in graben-like structures. We have studied two models, an idealized cylindrical graben and a scale model (1 mm to 1 km) of the Yucca Flat basin excavated into a halfspace of fine-grained gabbro and filled with low-velocity material.

Ultrasonic waves were excited on the surface of the model basin using a breaking pencil lead as a source; this source represents a step-function point unloading of the surface. The waves have been monitored using a true displacement conical transducer placed on the gabbro halfspace outside the basin, 200 mm away. Rayleigh waves of 40-120 kHz in the model correspond roughly to Rayleigh waves of period 20 s in the Earth, depending on the model and the fill material.

First, we made measurements setting the source off on the halfspace (made of gabbro, with V_p = 6.2 km/s), and within a cylindrical "graben" of 13 mm diameter and 2 mm depth. The graben was filled with either Crystalbond 504' (V_p = 2.407) or HPAL3 (V_p = 3.287). The presence of a source region with significantly slower velocities than the surrounding region appears to lead to a more complex signal, with more "ringing" than would be apparent if there were no such source region. The presence of such a source region appears to result in a relative amplification of the high-frequency part of the signal. The frequencies analogous to 3-10 s in the Earth appear to be amplified relative to lower frequencies. When the source is set off in the graben in an off-center position, a radiation pattern is established, with amplitude varying by a factor of 2 or more. Material effects appear to be accentuated when the source is excited off-center.

In the case of the more realistic scale model of Yucca Flat, the presence of the basin was also found to have an effect on the waveforms obtained. Some ringing and complexity are introduced into the waveforms, compared with waveforms obtained on a halfspace without a basin present. However, the effects are less dramatic than those observed when sources are excited on a model basin which is perfectly cylindrical in geometry. The most complex waveforms are obtained when the source is excited over the deepest portion of the graben. Here, we see some of the same kind of complexity and ringing observed in the cylindrical plug graben. When the source is anywhere within a rectangular box, representing the location of many actual explosions (Figs. 18-20), the effects are much less pronounced; the waveforms appear almost like halfspace responses.

The presence of the basin can cause some amplification of higher frequencies. Frequencies higher than about 400 kHz, which correpond roughly to periods of 2 s or shorter in the Earth, appear to be amplified relative to lower frequencies. This effect is most pronounced when the source is in the southern portion of the basin, as compared to the case when it is in the northern portion. The data also suggest an additional enhancement of this effect for wave propagation directions to the northwest or southeast.

In the real Earth, Yucca Flat is not embedded in a homogeneous halfspace, but in a more complex multilayered structure, and this may have a significant effect on seismic waveforms. It would be beneficial to conduct experiments involving grabens embedded in multilayered structures.

Clearly, a breaking pencil lead is a different source from a nuclear explosion, and although it is well characterized and useful in experiments such as these, it is not an exact model of a bomb. Thus, some caution should be exercised in the interpretation of these results.

8. Acknowledgements

The authors gratefully acknowledge Jim Bulau and Larry Bivins for assistance in the laboratory and for discussions; B.J. Hosten for providing certain ultrasonic velocity measurements; and Lloyd Graham for helpful discussions on ultrasonic sources and receivers.

9. References

Boler, F.M., Spetzler, H.A. and Getting, I.C., "Capacitance Transducer with a Point-Like Probe for Receiving Acoustic Emissions," Rev. Sci. Instrum. 55, 1293-1297 (1984).

Breckenridge, F.R., Tschiegg, C.E. and Greenspan, M., "Acoustic Emission: Some Applications of Lamb's Problem," J. Acoust. Soc. Am. 57, 626-631 (1975).

Ferguson, J.F., Felch, R.N., Aiken, C.V., Oldow, J.S. and Dockery, H., "Models of the Bouguer Gravity and Geologic Structure at Yucca Flat, Nevada," Geophysics 53, 2 (1988).

Hsu, N.N. and Hardy, S.C., "Experiments in Acoustic Emission Waveform Analysis for Characterization of AE Sources, Sensors, and Structures," in "Elastic Waves and Nondestructive Testing of Materials," ASME, AMD 29, 85-106 (1978).

McLaughlin, K.L., Anderson, L.M. and Lees, A.C., "Effects of Local Geologic Structure for Yucca Flats, NTS, Explosion Waveforms: 2-Dimensional Finite Difference Simulations," AFGL-TR-86-0220, Air Force Geophysics Laboratory, Hanscom AFB, MA, ADA179189.

Miklowitz, J., "The Theory of Elastic Waves and Waveguides," North Holland, New York, 618 (1978).

Mooney, H.M., "Some Numerical Solutions for Lamb's Problem," Bull. Seismol. Soc. Am. 64, 473-491 (1974).

Proctor, T.J., "Improved Piezoelectric Transducers for Acoustic Emission Reception," J. Acoust Soc. Am. 68, S68 (1980).

Proctor, T.J., "Some Details on the NBS Conical Transducer," J. Acoustic Emission 1, 173-178 (1982a).

Proctor, T.J., "An Improved Piezoelectric Acoustic Emission Transducer, J. Acoust. Soc. Am. 71, 1163-1168 (1982b).

Regan, J. and Glover, P., "Modeling Surface Waves in Laterally Heterogeneous Media," Proc. DARPA/AFGL Seismic Research Symposium, US Air Force Academy, Colorado Springs CO, May 6-8 1985.

Vassiliou, M.S., Abdel-Gawad, M., and Tittmann, B.R. (1986), "Ultrasonic Physical Modeling of Seismic Wave Propagation from a Graben-Like Structure: A Preliminary Report," AFGL-TR-86-0228, Air Force Geophysics Laboratory, Hanscom AFB, MA, ADA178396.

Vassiliou, M.S., Abdel-Gawad, M., and Tittmann, B.R. (1987), "Ultrasonic Physical Modeling of Seismic Wave Propagation from a Graben-Like Structure", paper presented at the Seismological Society of America Annual Meeting, March 25, 1987, University of California, Santa Barbara.

DISTRIBUTION LIST

Dr. Monem Abdel-Gawad
Rockwell Internat'l Science Center
1049 Camino Dos Rios
Thousand Oaks, CA 91360

Professor Keiiti Aki
Center for Earth Sciences
University of Southern California
University Park
Los Angeles, CA 90089-0741

Dr. Raplh Alewine III
DARPA/STO/GSD
1400 Wilson Boulevard
Arlington, CA 22209-2308

Professor Shelton S. Alexander
Geosciences Department
403 Deike Building
The Pennsylvania State University
University Park, PA 16802

Professor Charles B. Archambeau
Cooperative Institute for Resch
in Environmental Sciences
University of Colorado
Boulder, CO 80309

Dr. Thomas C. Bache Jr.
Science Applications Int'l Corp.
10210 Campus Point Drive
San Diego, CA 92121

Dr. Robert Blandford
DARPA/STO/GSD
1400 Wilson Boulevard
Arlington, CA 22209-2308

Dr. Lawrence Braile
Department of Geosciences
Purdue University
West Lafayette, IN 47907

Dr. James Bulau
Rockwell Int'l Science Center
1049 Camino Dos Rios
P.O. Box 1085
Thousand Oaks, CA 91360

Dr. Douglas R. Baumgardt
Signal Analysis & Systems Div.
ENSCO, Inc.
5400 Port Royal Road
Springfield, VA 22151-2388

Dr. G. Blake
US Dept of Energy/DP 331
Forrestal Building
1000 Independence Ave.
Washington, D.C. 20585

Dr. S. Bratt
Science Applications Int'l Corp.
10210 Campus Point Drive
San Diego, CA 92121

Woodward-Clyde Consultants
ATTN: Dr. Lawrence J. Burdick
Dr. Jeff Barker
P.O. Box 93245
Pasadena, CA 91109-3245 (2 copies)

Dr. Roy Burger
1221 Serry Rd.
Schenectady, NY 12309

Professor Robert W. Clayton
Seismological Laboratory/Div. of
Geological & Planetary Sciences
California Institute of Technology
Pasadena, CA 91125

Dr. Vernon F. Cormier/Earth Resources
Lab, Dept of Earth, Atmospheric and
Planetary Sciences
MIT - 42 Carleton Street
Cambridge, MA 02142

Professor Anton W. Dainty
AFGL/LWH
Hanscom AFB, MA 01731

Dr. Zoltan A. Der
ENSCO, Inc.
5400 Port Royal Road
Springfield, VA 22151-2388

Professor Adam Dziewonski
Hoffman Laboratory
Harvard University
20 Oxford St.
Cambridge, MA 02138

Professor John Ebel
Dept of Geology & Geophysics
Boston College
Chestnut Hill, MA 02167

Dr. Jack Evernden
USGS-Earthquake Studies
345 Middlefield Road
Menlo Park, CA 94025

Professor John Ferguson
Center for Lithospheric Studies
The University of Texas at Dallas
P.O. Box 830688
Richardson, TX 75083-0688

Mr. Edward Giller
Pacific Seirra Research Corp.
1401 Wilson Boulevard
Arlington, VA 22209

Dr. Jeffrey W. Given
Sierra Geophysics
11255 Kirkland Way
Kirkland, WA 98033

Professor Steven Grand
Department of Geology
245 Natural History Building
1301 West Green Street
Urbana, IL 61801

Professor Roy Greenfield
Geosciences Department
403 Deike Building
The Pennsylvania State University
University Park, PA 16802

Dr. James Hannon
Lawrence Livermore Nat'l Lab.
P.O. Box 808
Livermore, CA 94550

Professor David G. Harkrider
Seismological Laboratory
Div of Geological & Planetary Sciences
California Institute of Technology
Pasadena, CA 91125

Professor Donald V. Helmberger
Seismological Laboratory
Div of Geological & Planetary Sciences
California Institute of Technology
Pasadena, CA 91125

Professor Eugene Herrin
Institute for the Study of Earth
& Man/Geophysical Laboratory
Southern Methodist University
Dallas, TX 75275

Professor Robert B. Herrmann
Department of Earth & Atmospheric
Sciences
Saint Louis University
Saint Louis, MO 63156

U.S. Arms Control & Disarm. Agency
ATTN: Mrs. M. Hoinkes
Div. of Multilateral Affairs
Room 5499
Washington, D.C. 20451

Professor Lane R. Johnson
Seismographic Station
University of California
Berkeley, CA 94720

Professor Thomas H. Jordan
Department of Earth, Atmospheric
and Planetary Sciences
Mass Institute of Technology
Cambridge, MA 02139

Dr. Alan Kafka
Department of Geology &
Geophysics
Boston College
Chestnut Hill, MA 02167

Ms. Ann Kerr
DARPA/STO/GSD
1400 Wilson Boulevard
Arlington, VA 22209-2308

Professor Charles A. Langston
Geosciences Department
403 Deike Building
The Pennsylvania State University
University Park, PA 16802

Professor Thorne Lay
Department of Geological Sciences
1006 C.C. Little Building
University of Michigan
Ann Harbor, MI 48109-1063

Dr. Arthur Lerner-Lam
Lamont-Doherty Geological Observatory
of Columbia University
Palisades, NY 10964

Dr. George R. Mellman
Sierra Geophysics
11255 Kirkland Way
Kirkland, WA 98033

Professor Brian J. Mitchell
Department of Earth & Atmospheric
Sciences
Saint Louis University
Saint Louis, MO 63156

Professor Thomas V. McEvilly
Seismographic Station
University of California
Berkeley, CA 94720

Dr. Keith L. McLaughlin
Teledyne Geotech
314 Montgomery Street
Alexandria, VA 22314

Mr. Jack Murphy - S-CUBED
Reston Geophysics Office
11800 Sunrise Valley Drive
Suite 1212
Reston, VA 22091

Dr. Carl Newton
Los Alamos National Lab.
P.O. Box 1663
Mail Stop C335, Group E553
Los Alamos, NM 87545

Professor Otto W. Nuttli
Department of Earth &
Atmospheric Sciences
Saint Louis University
Saint Louis, MO 63156

Professor J. A. Orcutt
Geological Sciences Div.
Univ. of California at
San Diego
La Jolla, CA 92093

Dr. Frank F. Pilotte
Director of Geophysics
Headquarters Air Force Technical
Applications Center
Patrick AFB, Florida 32925-6001

Professor Keith Priestley
University of Nevada
Mackay School of Mines
Reno, Nevada 89557

Mr. Jack Raclin
USGS - Geology, Rm 3 C136
Mail Stop 928 National Center
Reston, VA 22092

Professor Paul G. Richards
Lamont-Doherty Geological
Observatory of Columbia Univ.
Palisades, NY 10964

Dr. Norton Rimer
S-CUBED
A Division of Maxwell Lab
P.O. 1620
La Jolla, CA 92038-1620

Dr. George H. Rothe
Chief, Research Division
Geophysics Directorate
HQ Air Force Technical
Applications Center
Patrick AFB, Florida 32925-6001

Professor Larry J. Ruff
Department of Geological Sciences
1006 C.C. Little Building
University of Michigan
Ann Arbor, MI 48109-1063

Dr. Alan S. Ryall, Jr.
Center of Seismic Studies
1300 North 17th Street
Suite 1450
Arlington, VA 22209-2308

Professor Charles G. Sammis
Center for Earth Sciences
University of Southern California
University Park
Los Angeles, CA 90089-0741

Dr. David G. Simpson
Lamont-Doherty Geological Observ.
of Columbia University
Palisades, NY 10964

Dr. Jeffrey L. Stevens
S-CUBED,
A Division of Maxwell Laboratory
P.O. Box 1620
La Jolla, CA 92038-1620

Professor Brian Stump
Institute for the Study of Earth & Man
Geophysical Laboratory
Southern Methodist University
Dallas, TX 75275

Professor Ta-liang Teng
Center for Earth Sciences
University of Southern California
University Park
Los Angeles, CA 90089-0741

Dr. R. B. Tittmann
Rockwell International Science Ctr
1049 Camino Dos Rios
P.O. Box 1085
Thousand Oaks, CA 91360

Professor M. Nafi Toksoz/Earth Resources
Lab - Dept of Earth, Atmospheric and
Planetary Sciences
MIT - 42 Carleton Street
Cambridge, MA 02142

Dr. Lawrence Turnbull
OSWR/NED
Central Intelligence Agency
CIA, Room 5G48
Washington, D.C. 20505

Professor Terry C. Wallace
Department of Geosciences
Building #11
University of Arizona
Tucson, AZ 85721

Professor John H. Woodhouse
Hoffman Laboratory
Harvard University
20 Oxford St.
Cambridge, MA 02138

***

DARPA/PM
1400 Wilson Boulevard
Arlington, VA 22209

Defense Technical
Information Center
Cameron Station
Alexandria, VA 22314
(12 copies)

Defense Intelligence Agency
Directorate for Scientific &
Technical Intelligence
Washington, D.C. 20301

Defense Nuclear Agency/SPSS
ATTN: Dr. Michael Shore
6801 Telegraph Road
Alexandria, VA 22310

AFOSR/NPG
ATTN: Director
Bldg 410, Room C222
Bolling AFB, Wash D.C. 20332

AFTAC/CA (STINFO)
Patrick AFB, FL 32925-6001

U.S. Geological Survey
ATTN: Dr. T. Hanks
Nat'l Earthquake Resch Center
345 Middlefield Road
Menlo Park, CA 94025

SRI International
333 Ravensworth Avenue
Menlo Park, CA 94025

Center for Seismic Studies
ATTN: Dr. C. Romney
1300 North 17th St., Suite 1450
Arlington, VA 22209 (3 copies)

Science Horizons, Inc.
ATTN: Dr. Bernard Minster
Dr. Theodore Cherry
710 Encinitas Blvd., Suite 101
Encinitas, CA 92024 (2 copies)

Dr. G. A. Bollinger
Department of Geological Sciences
Virginia Polytechnical Institute
21044 Derring Hall
Blacksburg, VA 24061

Dr. L. Sykes
Lamont Doherty Geological Observ.
Columbia University
Palisades, NY 10964

Dr. S. W. Smith
Geophysics Program
University of Washington
Seattle, WA 98195

Dr. L. Timothy Long
School of Geophysical Sciences
Georgia Institute of Technology
Atlanta, GA 30332

Dr. N. Biswas
Geophysical Institute
University of Alaska
Fairbanks, AK 99701

Dr. Freeman Gilbert - Institute of Geophysics & Planetary Physics
Univ. of California at San Diego
P.O. Box 109
La Jolla, CA 92037

Dr. Pradeep Talwani
Department of Geological Sciences
University of South Carolina
Columbia, SC 29208

Dr. Donald Forsyth
Dept. of Geological Sciences
Brown University
Providence, RI 02912

Dr. Jack Oliver
Department of Geology
Cornell University
Ithaca, NY 14850

Dr. Muawia Barazangi
Geological Sciences
Cornell University
Ithaca, NY 14853

Rondout Associates
ATTN: Dr. George Sutton,
Dr. Jerry Carter, Dr. Paul Pomeroy
P.O. Box 224
Stone Ridge, NY 12484 (3 copies)

Dr. Bob Smith
Department of Geophysics
University of Utah
1400 East 2nd South
Salt Lake City, UT 84112

Dr. Anthony Gangi
Texas A&M University
Department of Geophysics
College Station, TX 77843

Dr. Gregory B. Young
ENSCO Inc.
5400 Port Royal Road
Springfield, CA 22151

Weidlinger Associates
ATTN: Dr. Gregory Wojcik
620 Hansen Way, Suite 100
Palo Alto, CA 94304

Dr. Leon Knopoff
University of California
Institute of Geophysics
& Planetary Physics
Los Angeles, CA 90024

Dr. Kenneth H. Olsen
Los Alamos Scientific Lab.
Post Office Box 1663
Los Alamos, NM 87545

Professor Jon F. Claerbout
Professor Amos Nur
Dept. of Geophysics
Stanford University
Stanford, CA 94305 (2 copies)

Dr. Robert Burridge
Schlumberger-Doll Resch Ctr.
Old Quarry Road
Ridgefield, CT 06877

Dr. Robert Phinney/Dr. F.A. Dahlen
Dept of Geological
  Geophysical Sci. University
Princeton University
Princeton, NJ 08540 (2 copies)

New England Research, Inc.
ATTN: Dr. Randolph Martin III
P.O. Box 857
Norwich, VT 05055

Sandia National Laboratory
ATTN: Dr. H. B. Durham
Albuquerque, NM 87185

AFGL/XO
Hanscom AFB, MA 01731-5000

AFGL/LW
Hanscom AFB, MA 01731-5000

AFGL/SULL
Research Library
Hanscom AFB, MA 01731-5000 (2 copies)

Secretary of the Air Force (SAFRD)
Washington, DC 20330

Office of the Secretary Defense
DDR & E
Washington, DC 20330

HQ DNA
ATTN: Technical Library
Washington, DC 20305

Director, Technical Information
DARPA
1400 Wilson Blvd.
Arlington, VA 22209

Los Alamos Scientific Laboratory
ATTN: Report Library
Post Office Box 1663
Los Alamos, NM 87544

Dr. Thomas Weaver
Los Alamos Scientific Laboratory
Los Almos, NM 97544

Dr. Gary McCartor
Mission Research Corp.
735 State Street
P.O. Drawer 719
Santa Barbara, CA 93102

Dr. Al Florence
SRI International
333 Ravenwood Avenue
Menlo Park, CA 94025-3493

Dr. W. H. K. Lee
USGS
Office of Earthquakes, Volcanoes,
& Engineering
Branch of Seismology
345 Middlefield Rd
Menlo Park, CA 94025

***

Dr. Peter Basham/Earth Physics Branch
Department of Energy and Mines
1 Observatory Crescent
Ottawa, Ontario
CANADA K1A OY3

Dr. Eduard Berg
Institute of Geophysics
University of Hawaii
Honolulu, HI 96822

Dr. Michel Bouchon - Universite
Scientifique et Medicale de Grenob
Lab de Geophysique - Interne et
Tectonophysique - I.R.I.G.M-B.P.
38402 St. Martin D'Heres
Cedex FRANCE

Dr. Hilmar Bungum/NTNF/NORSAR
P.O. Box 51
Norwegian Council of Science,
Industry and Research, NORSAR
N-2007 Kjeller, NORWAY

Dr. Kin-Yip Chun
Geophysics Division
Physics Department
University of Toronto
Ontario, CANADA M5S 1A7

Dr. Alan Douglas
Ministry of Defense
Blacknest, Brimpton,
Reading RG7-4RS
UNITED KINGDOM

Professor Peter Harjes
Institute for Geophysik
Rhur University/Bochum
P.O. Box 102148, 4630 Bochum 1
FEDERAL REPUBLIC OF GERMANY

Dr. E. Husebye
NTNF/NORSAR
P.O. Box 51
N-2007 Kjeller, NORWAY

Mr. Peter Marshall, Procurement
Executive, Ministry of Defense
Blacknest, Brimpton,
Reading FG7-4RS
UNITED KINGDOM

Dr. B. Massinon
Societe Radiomana
27, Rue Claude Bernard
75005, Paris, FRANCE

Dr. Pierre Mechler
Societe Radiomana
27, Rue Claude Bernard
75005, Paris, FRANCE

Dr. Ben Menaheim
Weizman Institute of Science
Rehovot, ISRAEL 951729

Dr. Svein Mykkeltveit
NTNF/NORSAR
P.O. Box 51
N-2007 Kjeller, NORWAY

Dr. Frode Ringdal
NTNF/NORSAR
P.O. Box 51
N-2007 Kjeller, NORWAY

University of Hawaii
Institute of Geophysics
ATTN: Dr. Daniel Walker
Honolulu, HI 96822

***